Model-independent constraints on new physics in $b \rightarrow s$ transitions

Wolfgang Altmannshofer,[a] **Paride Paradisi**[b] **and David M. Straub**[c]

[a]*Fermi National Accelerator Laboratory,*
P.O. Box 500, Batavia, IL 60510, U.S.A.

[b]*Theory Division, CERN,*
CH-1211, Geneva 23, Switzerland

[c]*Scuola Normale Superiore and INFN,*
Piazza dei Cavalieri 7, 56126 Pisa, Italy

E-mail: waltmann@fnal.gov, paride.paradisi@cern.ch,
david.straub@sns.it

Abstract: We provide a comprehensive model-independent analysis of rare decays involving the $b \rightarrow s$ transition to put constraints on dimension-six $\Delta F = 1$ effective operators. The constraints are derived from all the available up-to-date experimental data from the B-factories, CDF and LHCb. The implications and future prospects for observables in $b \rightarrow s\ell^+\ell^-$ and $b \rightarrow s\nu\bar{\nu}$ transitions in view of improved measurements are also investigated. The present work updates and generalises previous studies providing, at the same time, a useful tool to test the flavour structure of any theory beyond the SM.

Contents

1 Introduction

The CKM description of flavour and CP violation in the Standard Model (SM) has been extremely successful in describing the data from high-precision flavour experiments, among them the B factories and the Tevatron, and is also in agreement with recent measurements of rare B decays at LHC. This is a remarkable fact, given that the origin of flavour, i.e. the origin of the replication of fermion species and of the hierarchies in their masses and mixing is still a complete mystery. If one supposes new physics (NP) to be at work not too far above the electroweak scale, as is implied by the gauge hierarchy problem, this fact is even more surprising, since NP coupling to the SM generally leads to modifications of flavour violation, in particular in flavour-changing neutral current (FCNC) processes, which are suppressed by the GIM mechanism and arise only at the loop level in the SM. Even under the most restrictive of assumptions that can be made on the flavour sector of a NP theory, namely assuming all flavour violation to be governed by the SM Yukawa couplings (the hypothesis of Minimal Flavour Violation [1, 2], MFV), many models predict significant deviations in FCNC observables. Moreover, many of the flavour-violating couplings are rather poorly constrained as yet and still allow for sizable NP contributions. In $\Delta B = 1$ transitions, this is particularly true for NP contributions with a different CP phase or chirality with respect to the SM contribution. In that case, large deviations in observables *not* measured yet are still easily possible. Quantifying this statement is one of the main goals of this paper.

Experimentally, the prospects to improve constraints on flavour violating couplings are excellent: Today, the LHCb experiment has a high sensitivity to exclusive hadronic, semi-leptonic and leptonic B and B_s decays [3].[1] In the mid-term future, two next-generation B factories will allow also the measurement of inclusive rare decays and decays with neutrinos in the final state [4, 5].

Since FCNC processes test NP indirectly, through quantum corrections induced by heavy particles, the impact of NP on low-energy observables like branching ratios or asymmetries can be summarised by their modification of Wilson coefficients of local, non-renormalizable operators. These short-distance coefficients can be constrained on a completely model-independent basis by measuring FCNC observables and these constraints can in turn be used to constrain individual NP models.

In this paper, we concentrate on $\Delta B = \Delta S = 1$ processes, i.e. rare decays with a $b \to s$ transition. We use up-to-date experimental constraints — in particular, we include the recent measurement at LHCb of angular observables in $B \to K^* \mu^+ \mu^-$ [6], which is the most precise to date — to put model-independent constraints on the Wilson coefficients.[2] Similar constraints have been considered in the literature before, e.g. in the context of MFV [9–11], magnetic penguin operators [12], SM operators [13–15] or generic

---

[1]In the case of leptonic decays, also ATLAS and CMS are competitive.

[2]Instead, we do not consider here observables related to the decay $B \to K\ell^+\ell^-$, since their current experimental resolutions are rather poor. Including them would affect our results only in a negligible way. However, once LHCb data on $B \to K\ell^+\ell^-$ observables will become available, it will be important to include them given their high NP sensitivity [7, 8].

NP [16–18]. We generalise these studies by considering SM operators, their chirality-flipped counterparts and generic CP violation and considering also the case where they are all simultaneously present instead of considering only a pair at a time. After imposing the above constraints, we investigate the room left for NP in observables which have not been measured yet, like the branching ratios of $B_s \to \mu^+\mu^-$ and $B_s \to \tau^+\tau^-$, CP asymmetries in $B \to K^*\mu^+\mu^-$ and observables in $b \to s\nu\bar{\nu}$ decays.

The paper is organised as follows. In section 2, we specify the effective Hamiltonian for $b \to s$ transitions and discuss all the observables relevant for our study. In section 3, we present our numerical results for the model-independent constraints on the Wilson coefficients. In section 4, we consider the constraints in the more restrictive case of semi-leptonic operators generated dominantly by modified Z couplings, which is the case in many models beyond the SM. This allows us to correlate $b \to s\ell^+\ell^-$ processes to $b \to s\nu\bar{\nu}$ processes. Our main findings are summarised in section 5.

2 Observables in $b \to s\gamma$ and $b \to s\ell^+\ell^-$ decays

The effective Hamiltonian relevant for $b \to s\gamma$ and $b \to s\ell^+\ell^-$ transitions is given by [19, 20]

$$\mathcal{H}_{\text{eff}} = -\frac{4\,G_F}{\sqrt{2}} V_{tb} V_{ts}^* \frac{e^2}{16\pi^2} \sum_i (C_i O_i + C_i' O_i') + \text{h.c.} . \qquad (2.1)$$

The operators O_i that are most sensitive to NP effects are

$$
\begin{aligned}
O_7 &= \frac{m_b}{e}(\bar{s}\sigma_{\mu\nu}P_R b)F^{\mu\nu}, & O_8 &= \frac{gm_b}{e^2}(\bar{s}\sigma_{\mu\nu}T^a P_R b)G^{\mu\nu\,a}, \\
O_9 &= (\bar{s}\gamma_\mu P_L b)(\bar{\ell}\gamma^\mu\ell), & O_{10} &= (\bar{s}\gamma_\mu P_L b)(\bar{\ell}\gamma^\mu\gamma_5\ell), \\
O_S &= m_b(\bar{s}P_R b)(\bar{\ell}\ell), & O_P &= m_b(\bar{s}P_R b)(\bar{\ell}\gamma_5\ell),
\end{aligned}
\qquad (2.2)
$$

where m_b denotes the running b quark mass in the $\overline{\text{MS}}$ scheme and $P_{L,R} = (1 \mp \gamma_5)/2$. The corresponding operators O_i' are obtained from the operators O_i via the replacement $P_L \leftrightarrow P_R$. Numerical values of the Wilson coefficients and the relation of the coefficients at the matching scale to the effective low-energy coefficients are discussed in appendix B.

Note that we assume $C_9^{(\prime)}$ and $C_{10}^{(\prime)}$ to be independent of the lepton flavour, but $C_S^{(\prime)}$ and $C_P^{(\prime)}$ to be proportional to the lepton Yukawa couplings (this assumption will become relevant when we discuss the relation between $B_s \to \mu^+\mu^-$ and $B_s \to \tau^+\tau^-$). Moreover, we also assume lepton flavour conservation, which is an excellent approximation for our purposes, given the stringent experimental bounds on lepton flavour violating processes.

We will now discuss the observables in processes sensitive to this effective Hamiltonian, which can be used to constrain new physics.

2.1 $B_s \to \ell^+\ell^-$

In the SM, the $B_s \to \mu^+\mu^-$ decay is strongly helicity suppressed and among the rarest FCNC decays. Using directly the value of the B_s meson decay constant from the lattice,

$f_{B_s} = (250 \pm 12) \, \text{MeV}$ [21] we get the following SM prediction[3]

$$\text{BR}(B_s \to \mu^+\mu^-)_{\text{SM}} = (3.7 \pm 0.4) \times 10^{-9} \,. \tag{2.3}$$

The LHCb and CMS collaborations have set a combined upper bound on the branching ratio of [24–26]

$$\text{BR}(B_s \to \mu^+\mu^-)_{\text{LHC}} < 1.1 \times 10^{-8} \tag{2.4}$$

at 95% confidence level.[4]

In a generic NP model, the branching ratio of $\text{BR}(B_s \to \mu^+\mu^-)$ is given by

$$\frac{\text{BR}(B_s \to \mu^+\mu^-)}{\text{BR}(B_s \to \mu^+\mu^-)_{\text{SM}}} = |S|^2 \left(1 - \frac{4m_\mu^2}{m_{B_s}^2}\right) + |P|^2, \tag{2.5}$$

where

$$S = \frac{m_{B_s}^2}{2m_\mu} \frac{(C_S - C_S')}{|C_{10}^{\text{SM}}|}, \qquad P = \frac{m_{B_s}^2}{2m_\mu} \frac{(C_P - C_P')}{C_{10}^{\text{SM}}} + \frac{(C_{10} - C_{10}')}{C_{10}^{\text{SM}}}. \tag{2.6}$$

The important feature of $B_s \to \mu^+\mu^-$ as a probe of NP is that it is among the very few $b \to s$ decays that are strongly sensitive to scalar and pseudoscalar operators. In models where such operators are sizable, the branching ratio can easily saturate the experimental limit. In section 3, we will use measurements of other $b \to s$ processes to constrain the Wilson coefficients $C_{10}^{(\prime)}$, which then allows us to predict the maximum allowed size of $\text{BR}(B_s \to \mu^+\mu^-)$ *in the absence* of (pseudo)scalar currents.

The process $B_s \to \tau^+\tau^-$, is governed by Wilson coefficients analogous to $B_s \to \mu^+\mu^-$ and its branching ratio is given by eqs. (2.5) and (2.6) with the appropriate replacement $\mu \to \tau$.

2.2 $b \to s\gamma$

The experimental data on the branching ratio of the inclusive $B \to X_s\gamma$ decay [28]

$$\text{BR}(B \to X_s\gamma)_{\text{exp}} = (3.55 \pm 0.26) \times 10^{-4} \,, \tag{2.7}$$

and the corresponding NNLO SM prediction [29, 30]

$$\text{BR}(B \to X_s\gamma)_{\text{SM}} = (3.15 \pm 0.23) \times 10^{-4} \,, \tag{2.8}$$

show good agreement. As the $\text{BR}(B \to X_s\gamma)$ is highly sensitive to NP contributions to the Wilson coefficients $C_7^{(\prime)}$, this agreement leads to severe constraints on the flavour sectors of many NP models. In our numerical analysis, we use the expression for the branching ratio reported in [31], rescaled to the SM prediction of [29], and assume the uncertainty in the SM prediction as relative error on the theory prediction.

---

[3]Using the remarkably precise value for f_{B_s} obtained very recently in [22]: $f_{B_s} = (225 \pm 4) \, \text{MeV}$, we obtain $\text{BR}(B_s \to \mu^+\mu^-)_{\text{SM}} = (3.0 \pm 0.2) \times 10^{-9}$. This result is as precise as the value that is obtained by assuming ΔM_s free of NP and using its measurement to reduce the theory uncertainty in $B_s \to \mu^+\mu^-$ arising from the B_s meson decay constant [23]. However, to be conservative, we use (2.3) in our analysis.

[4]We mention that the CDF collaboration found an excess of candidates for $B_s \to \mu^+\mu^-$ decays, which have been used to determine [27] $\text{BR}(B_s \to \mu^+\mu^-)_{\text{CDF}} = \left(1.8^{+1.1}_{-0.9}\right) \times 10^{-8}$.

Another interesting observable that probes the $b \to s\gamma$ transition is the time-dependent CP asymmetry in the exclusive $B_d \to K^*(\to K_S^0\pi^0)\gamma$ decay [32–35]

$$\frac{\Gamma(\bar{B}^0(t) \to \bar{K}^{*0}\gamma) - \Gamma(B^0(t) \to K^{*0}\gamma)}{\Gamma(\bar{B}^0(t) \to \bar{K}^{*0}\gamma) + \Gamma(B^0(t) \to K^{*0}\gamma)} = S_{K^*\gamma}\sin(\Delta M_d t) - C_{K^*\gamma}\cos(\Delta M_d t) . \quad (2.9)$$

The coefficient $S_{K^*\gamma}$ is highly sensitive to right handed currents as at leading order it vanishes for $C_7' \to 0$. As a consequence, SM contributions to $S_{K^*\gamma}$ are suppressed by m_s/m_b or $\Lambda_{\rm QCD}/m_b$ [33], resulting in a very small SM prediction [35]

$$S_{K^*\gamma}^{\rm SM} = (-2.3 \pm 1.6)\% . \quad (2.10)$$

Experimental evidence for a large $S_{K^*\gamma}$ would be a clear indication of NP effects through right handed currents. On the experimental side one has presently [28, 36, 37]

$$S_{K^*\gamma}^{\rm exp} = -0.16 \pm 0.22 \quad (2.11)$$

and the prospects to improve this measurement significantly at next generation B factories are excellent [38]. In our numerical analysis we use the LO expression for $S_{K^*\gamma}$ [34]

$$S_{K^*\gamma} \simeq \frac{2}{|C_7|^2 + |C_7'|^2}{\rm Im}\left(e^{-i\phi_d}C_7 C_7'\right) , \quad (2.12)$$

that leads to accurate predictions in presence of NP. In the above expression for $S_{K^*\gamma}$, $\sin(\phi_d) = S_{\psi K_S}$ is the phase of the B_d mixing amplitude and the Wilson coefficients are evaluated at the scale $\mu = m_b$. Using directly the experimental value for $S_{\psi K_S} = 0.67 \pm 0.02$ [28], we automatically capture possible NP effects in B_d mixing. In our NP analysis, we assume the theory uncertainty to be equal to the SM uncertainty in (2.10).

Another observable that is in principle sensitive to CP violating effects in the $b \to s\gamma$ transition is $A_{\rm CP}(b \to s\gamma)$, the direct CP asymmetry in the $B \to X_s\gamma$ decay [39, 40]. In contrast to the observables discussed so far, it is also highly sensitive to NP contributions to the Wilson coefficients $C_8^{(\prime)}$. However, as shown in [41], the SM prediction for $A_{\rm CP}(b \to s\gamma)$ is dominated by long-distance contributions and large hadronic uncertainties make it difficult to predict this observable reliably in the context of NP scenarios. We therefore do not consider $A_{\rm CP}(b \to s\gamma)$ in our analysis. We also do not consider the isospin asymmetry in $B \to K^*\gamma$, as large hadronic uncertainties strongly limit the constraining power of this observable.

2.3 $B \to X_s\ell^+\ell^-$

We consider the inclusive $B \to X_s\ell^+\ell^-$ decay in two different regions of the dilepton invariant mass. The low q^2 region with $1\,{\rm GeV}^2 < q^2 < 6\,{\rm GeV}^2$ and the high q^2 region with $q^2 > 14.4\,{\rm GeV}^2$. Averaging the available results from BaBar [42] and Belle [43] one finds the following averages for the branching ratios in the two regions

$${\rm BR}(B \to X_s\ell^+\ell^-)_{[1,6]}^{\rm exp} = (1.63 \pm 0.50)10^{-6}, \quad {\rm BR}(B \to X_s\ell^+\ell^-)_{>14.4}^{\rm exp} = (4.3 \pm 1.2)10^{-7}. \quad (2.13)$$

These results should be compared to the SM predictions [19, 44–51]

$$\mathrm{BR}(B \to X_s \ell^+ \ell^-)^{\mathrm{SM}}_{[1,6]} = (1.59 \pm 0.11)10^{-6}, \quad \mathrm{BR}(B \to X_s \ell^+ \ell^-)^{\mathrm{SM}}_{>14.4} = (2.3 \pm 0.7)10^{-7}. \quad (2.14)$$

While the low q^2 values are in perfect agreement, the SM prediction in the high q^2 region is on the low side of the experimental result. We remark that the theory prediction in the low q^2 region quoted above does not include effects from the experimental cut on the hadronic final state. Such effects can be as large as 10% [52, 53]. Enlarging the theory error correspondingly however would effect our results only in a minor way, given the huge experimental uncertainty in $\mathrm{BR}(B \to X_s \ell^+ \ell^-)$.

The branching ratio in the high q^2 region is mainly sensitive to NP contributions to the Wilson coefficients $C_9^{(\prime)}$ and $C_{10}^{(\prime)}$, while the branching ratio in the low q^2 region also depends strongly on $C_7^{(\prime)}$. In our numerical analysis, we use the expressions given in [11], adjusting them to take into account also the primed Wilson coefficients, and treat the uncertainties in the SM predictions as relative errors on the theory predictions.

In principle, another interesting observable to constrain NP would be the forward-backward asymmetry in $B \to X_s \ell^+ \ell^-$. However, since it has not been measured yet, we do not include it in our analysis. A fully inclusive measurement is probably not feasible at LHCb and it will only be possible at next generation B factories [5, 38, 54].

2.4 $B \to K^* \mu^+ \mu^-$

The angular distribution of the exclusive $\bar{B} \to \bar{K}^{*0}(\to K^- \pi^+)\mu^+ \mu^-$ decay gives access to many observables potentially sensitive to NP [14, 15, 17, 31, 55, 56, 61–65]. By means of its charge conjugated mode $B \to K^{*0}(\to K^+ \pi^-)\mu^+ \mu^-$, which can be distinguished from the former simply by the meson charges, this decay allows a straightforward measurement of CP asymmetries.

Neglecting scalar operator contributions (which are strongly constrained by $B_s \to \mu^+ \mu^-$) and lepton mass effects (which is a very good approximation for electrons and muons even if effects from collinear QED logarithms are taken into account [48]), the full set of observables accessible in the angular distribution of the decay and its CP-conjugate is given by 9+9 angular coefficients $I_i(q^2)$ and $\bar{I}_i(q^2)$, which are functions of the dilepton invariant mass q^2. While the overall normalization of the angular coefficients is subject to considerable uncertainties, theoretically cleaner observables are obtained by normalizing them to the total invariant mass distribution. Furthermore, it makes sense to separate the observables into CP asymmetries A_i and CP-averaged ones S_i. One thus arrives at [55]

$$S_i = \left(I_i + \bar{I}_i \right) \Big/ \frac{d(\Gamma + \bar{\Gamma})}{dq^2}, \qquad A_i = \left(I_i - \bar{I}_i \right) \Big/ \frac{d(\Gamma + \bar{\Gamma})}{dq^2}. \quad (2.15)$$

We will also consider observables integrated in a q^2 range, defined as

$$\langle S_i \rangle_{[a,b]} = \left(\int_a^b dq^2 \left(I_i + \bar{I}_i \right) \right) \Big/ \left(\int_a^b dq^2 \frac{d(\Gamma + \bar{\Gamma})}{dq^2} \right), \quad (2.16)$$

and analogously for $\langle A_i \rangle$.

For all observables one has to distinguish, both theoretically and experimentally, between the kinematical region where the dilepton invariant mass is below the charmonium resonances (low q^2 or large recoil region) and the region above (high q^2 or low recoil region). The intermediate region is of no interest to probe NP, as the $c\bar{c}$ resonances dominate the short distance rate by two orders of magnitude.

At low q^2, the observables are sensitive to all the Wilson coefficients $C_{7,9,10}^{(\prime)}$. Among the CP asymmetries,[5] the most promising ones are then the T-odd CP asymmetries A_7, A_8 and A_9, which are not suppressed by small strong phases [17]. At high q^2, the contributions of the magnetic penguin operators $C_7^{(\prime)}$ are suppressed, which in turn allows a cleaner sensitivity to the semi-leptonic operators. The CP asymmetries reduce to three independent ones, which are however T-even and therefore suppressed by small strong phases even beyond the SM [15]. Among the CP-averaged angular coefficients, two have already been measured [6, 57–60]: the forward-backward asymmetry $A_{\rm FB}$ and the K^* longitudinal polarisation fraction F_L. Recently, the CDF collaboration also published first bounds on S_3 and A_9 [60]. A promising observable in the early phase of LHC is the observable S_5 [67].

Since different notations and conventions exist for the numerous $B \to K^* \ell^+ \ell^-$ observables, in table 1 we provide a dictionary between the notation used in this work and a selection of other theory and experimental papers. It also lists the Wilson coefficients which, if modified by NP, would have the biggest impact on the observable in question. In the case of C_7 and C_7', this sensitivity is only present at low q^2.

The main challenge in the theoretical prediction of the $B \to K^* \ell^+ \ell^-$ observables is given on the one hand by the $B \to K^*$ form factors; on the other by non-factorisable effects.[6] At low q^2, QCD factorisation can be used in the heavy quark limit, which reduces the number of independent form factors from 7 to 2 and allows a systematic calculation of non-factorizable corrections [69, 70]. The remaining theoretical uncertainties then reside in phenomenological parameters like meson distribution amplitudes, in the form factors themselves, as well as in possible corrections of higher order in the ratio $\Lambda_{\rm QCD}/m_b$. Instead of using the two form factors in the heavy quark limit, we use the full set of seven form factors calculated by QCD sum rules on the light cone (LCSR), using the results of [55, 71]. This approach has two advantages. First, using the full set of form factors takes into account an important source of power suppressed corrections at low q^2. Second, the correlated uncertainties between the different form factors obtained from the LCSR calculation leads to a strongly reduced form factor uncertainty on observables involving ratios of form factors.

At high q^2, QCD factorization and LCSR methods are not applicable. For the form factors, lacking predictions from lattice QCD, one currently has to rely on extrapolations of low-q^2 calculations, which introduce considerable uncertainty. For the estimation of non-factorizable corrections, an operator product expansion in powers of $1/\sqrt{q^2}$ can be used [72, 73] and in ref. [73] it has been argued that non-perturbative corrections *not* accounted for by the form factors are of the order of only a few percent. We do take into

---

[5]We do not consider the CP asymmetries A_{6s}^{V2s} and A_8^V defined in [66] since the former is suppressed by a small strong phase even beyond the SM and the latter is normalized to the quantity $I_8 + \bar{I}_8$, which is zero at LO even beyond the SM and afflicted with considerable uncertainty.

[6]For a recent discussion of uncertainties in the low q^2 region see also [68].

Obs.	[55]	[56]	[17]	[57–59]	[60]	most sensitive to
F_L	$-S_2^c$	F_L		F_L	F_L	$C_{7,9,10}^{(\prime)}$
$A_{\rm FB}$	$\frac{3}{4}S_6^s$	$A_{\rm FB}$	$A_{\rm FB}$	$-A_{\rm FB}$	$-A_{\rm FB}$	C_7, C_9
S_5	S_5					C_7, C_7', C_9, C_{10}'
S_3	S_3	$\frac{1}{2}(1-F_L)A_T^{(2)}$			$\frac{1}{2}(1-F_L)A_T^{(2)}$	$C_{7,9,10}'$
A_9	A_9		$\frac{2}{3}A_9$		A_{im}	$C_{7,9,10}'$
A_7	A_7		$-\frac{2}{3}A_7^D$			$C_{7,10}^{(\prime)}$

Table 1. Dictionary between different notations for the $B \to K^* \mu^+ \mu^-$ observables and Wilson coefficients they are most sensitive to (the sensitivity to $C_7^{(\prime)}$ is only present at low q^2).

account non-factorizable corrections proportional to form factors at $O(\alpha_s)$ both at low and high q^2 [45, 51, 69, 70, 74].

For our numerical analysis, a description of our treatment of theory uncertainties in the $B \to K^* \mu^+ \mu^-$ observables is in order. For both high and low q^2, we take into account parametric uncertainties, varying the ratio m_c/m_b from 0.25 to 0.33, the renormalization scale from 4.0 to 5.6 GeV [55] and the CKM angle γ by $\pm 11°$ [75]. At low q^2, as mentioned above, we make use of the LCSR calculation of all 7 form factors and vary the LCSR parameters as discussed in ref. [55]. To be conservative, we add an additional real scale factor with an uncertainty of 10% to each of the transversity amplitudes to account for possible additional power suppressed corrections. The branching ratio is the only observable that is sensitive to the overall normalization of the form factors. Since LCSR only give predictions for the B meson decay constant times a form factor, we add an additional relative uncertainty of twice the uncertainty of $f_B = (205 \pm 12)$ MeV [21] to the branching ratio. Unlike in [55], we do not use the data on $B \to K^* \gamma$ to fix the form factor normalization, since we allow for NP also in $B \to K^* \gamma$. We add all the individual uncertainties in quadrature. At high q^2, we use the extrapolated form factors of ref. [76]. In the Simplified Series Expansion used there, each form factor depends on two parameters fitted to the low-q^2 LCSR calculation. We estimate the form factor uncertainty by varying all 14 fit parameters separately, i.e. considering the uncertainties of the individual form factors as uncorrelated to each other, and add the resulting errors in quadrature. We consider this approach to be conservative. In view of the resulting sizable form factor uncertainties, at high q^2 we do not consider additional uncertainties due to power corrections or duality violation, which should amount to only a few percent [73] and are therefore numerically irrelevant.

Figure 1 shows the predictions for F_L and $A_{\rm FB}$ with our error estimates at low and high q^2 and compares them to the experimental data from Belle [58], CDF [77] and LHCb [6]. We do not show the data from BaBar [57], since they are given in large bins that include q^2 regions which are under poor theoretical control.

3 Model-independent constraints on Wilson coefficients

In a vast class of models beyond the SM, all NP effects in the observables listed in table 2 and discussed in section 2 are described by a modification of the Wilson coefficients
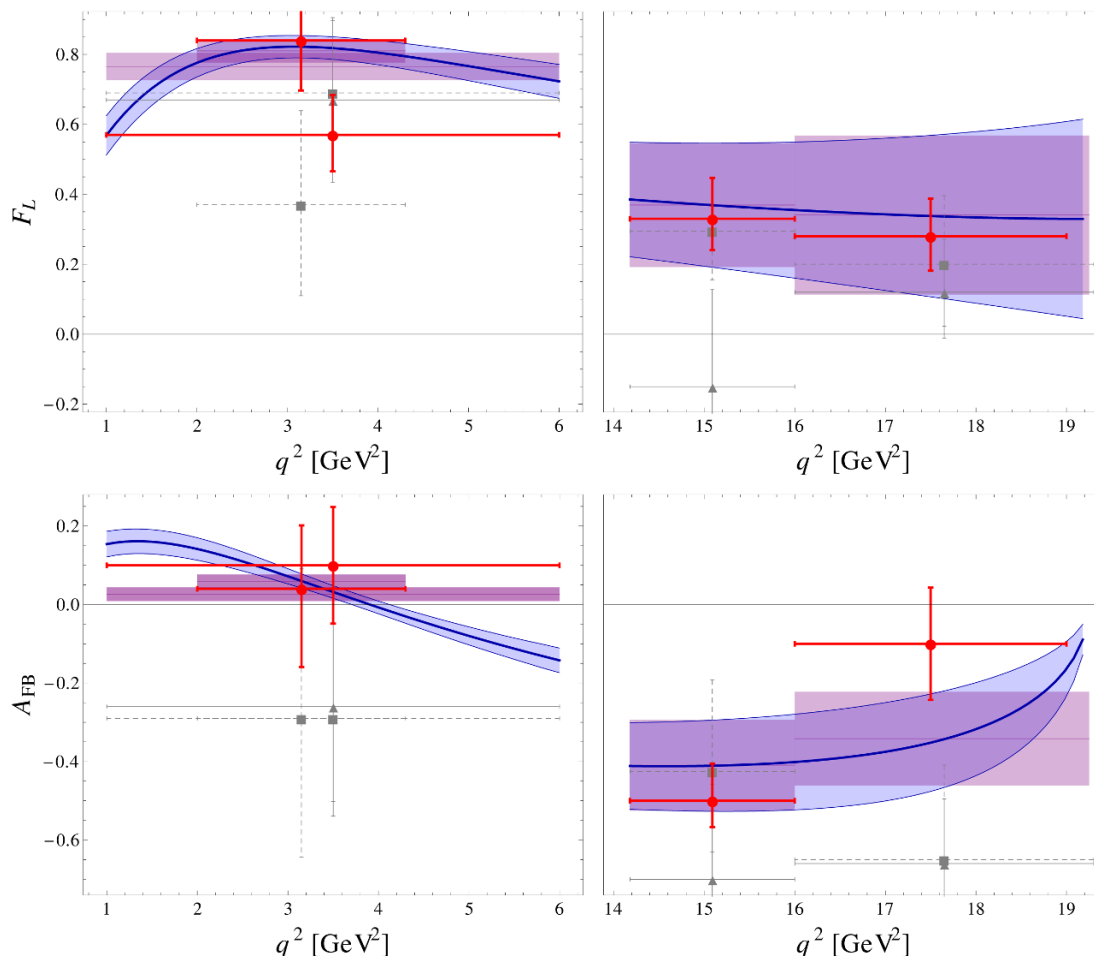
Figure 1. Theory prediction (blue bands), binned theory prediction (purple horizontal bands) and experimental measurements from LHCb (red dots, thick error bars), CDF (gray squares, dashed error bars) and Belle (gray triangles, solid error bars) for $A_{\rm FB}$ and F_L in $B \to K^* \mu^+ \mu^-$ for the two theoretically controllable q^2 regions.

$C^{(\prime)}_{7,8,9,10,S,P}$ at a matching scale, typically of the order of heavy particles contributing to the FCNC processes. For definiteness, we will consider in the following constraints on Wilson coefficients evaluated at the scale $\mu_h = 160\,{\rm GeV}$. The values at any other scale below the matching scale can be obtained straightforwardly using the renormalization group [78, 79], see also appendix B.

Up to subleading contributions, the coefficients $C^{(\prime)}_8$ enter the processes of interest only via renormalization group running by the mixing of the operators $\mathcal{O}^{(\prime)}_7$ and $\mathcal{O}^{(\prime)}_8$. Therefore, we will not consider constraints on $C^{(\prime)}_8$ in the following and keep in mind that, in the presence of $C^{(\prime)}_8$, the constraints on $C^{(\prime){\rm NP}}_7$ we present can be understood as constraints on the combination $(C^{(\prime){\rm NP}}_7 + 0.16\, C^{(\prime){\rm NP}}_8)$ at μ_h (see appendix B). Among the observables we consider, the scalar and pseudoscalar coefficients $C^{(\prime)}_{S,P}$ can only affect the branching ratios of $B_s \to \mu^+ \mu^-$ and $B_s \to \tau^+ \tau^-$ in a significant way. Thus, we will disregard also these coefficients and instead use the constraints on the remaining Wilson coefficients to give a

Observable	Experiment		SM prediction	
$10^4 \times \mathrm{BR}(B \to X_s \gamma)$	3.55 ± 0.26	[28]	3.15 ± 0.23	[29]
$S_{K^* \gamma}$	-0.16 ± 0.22	[28]	$(-2.3 \pm 1.6)\%$	[35]
$10^6 \times \mathrm{BR}(B \to X_s \ell^+ \ell^-)_{[1,6]}$	1.63 ± 0.50	[42, 43]	1.59 ± 0.11	[48]
$10^7 \times \mathrm{BR}(B \to X_s \ell^+ \ell^-)_{>14.4}$	4.3 ± 1.2	[42, 43]	2.3 ± 0.7	[11]
$10^7 \times \mathrm{BR}(B \to K^* \ell^+ \ell^-)_{[1,6]}$	1.71 ± 0.22	[6, 58, 77]	2.28 ± 0.63	
$10^7 \times \mathrm{BR}(B \to K^* \ell^+ \ell^-)_{[14.18,16]}$	1.11 ± 0.13	[6, 58, 77]	1.13 ± 0.33	
$10^7 \times \mathrm{BR}(B \to K^* \ell^+ \ell^-)_{[16,19]}$	1.35 ± 0.15	[6, 58, 77]	1.34 ± 0.51	
$\langle F_L \rangle (B \to K^* \ell^+ \ell^-)_{[1,6]}$	0.61 ± 0.09	[6, 58, 60]	0.77 ± 0.04	
$\langle F_L \rangle (B \to K^* \ell^+ \ell^-)_{[14.18,16]}$	0.28 ± 0.09	[6, 58, 60]	0.37 ± 0.17	
$\langle F_L \rangle (B \to K^* \ell^+ \ell^-)_{[16,19]}$	0.23 ± 0.08	[6, 58, 60]	0.34 ± 0.22	
$\langle A_{FB} \rangle (B \to K^* \ell^+ \ell^-)_{[1,6]}$	-0.04 ± 0.12	[6, 58, 60]	0.03 ± 0.02	
$\langle A_{FB} \rangle (B \to K^* \ell^+ \ell^-)_{[14.18,16]}$	-0.50 ± 0.07	[6, 58, 60]	-0.41 ± 0.11	
$\langle A_{FB} \rangle (B \to K^* \ell^+ \ell^-)_{[16,19]}$	-0.38 ± 0.10	[6, 58, 60]	-0.35 ± 0.11	
$\langle S_3 \rangle (B \to K^* \ell^+ \ell^-)_{[1,6]}$	0.27 ± 0.56	[60]	$(-0.3 \pm 1.1)\, 10^{-2}$	
$\langle A_9 \rangle (B \to K^* \ell^+ \ell^-)_{[1,6]}$	0.09 ± 0.39	[60]	$(1.5 \pm 2.4)\, 10^{-4}$	

Table 2. Experimental averages and SM predictions for the observables used in the fit.

prediction for the maximum possible sizes of $\mathrm{BR}(B_s \to \mu^+ \mu^-)$ and $\mathrm{BR}(B_s \to \tau^+ \tau^-)$ *in the absence* of (pseudo)scalar operators. We are thus left with the 6, potentially complex, Wilson coefficients $C_{7,9,10}^{(\prime)}$.

To obtain constraints on the Wilson coefficients, we construct a χ^2 function, which is a function of Wilson coefficients $\vec{C}$ and contains the theory predictions for the observables O_i^{th} and the experimental central values O_i^{exp} as well as the corresponding uncertainties (which we assume to be Gaussian),

$$\chi^2(\vec{C}) = \sum_i \frac{\left(O_i^{\mathrm{exp}} - O_i^{\mathrm{th}}(\vec{C})\right)^2}{(\sigma_i^{\mathrm{exp}})^2 + (\sigma_i^{\mathrm{th}}(\vec{C}))^2}. \tag{3.1}$$

We write the theory uncertainty as a function of Wilson coefficients since, as discussed in section 2, it is a relative error for some observables and for some others, such as the $B \to K^* \mu^+ \mu^-$ angular coefficients, can even be a non-trivial function of Wilson coefficients.

In table 2 we summarise the SM predictions as well as the experimental values of the observables that we use in the χ^2 function. To obtain the experimental values we perform weighted averages of the available measurements, symmetrising the errors using the prescription of ref. [80].

3.1 Impact of observables on pairs of Wilson coefficients

Using the χ^2 function, we can obtain constraints on the real or imaginary parts of a pair of Wilson coefficients, or in the complex plane of a single Wilson coefficient. This approach, which is reminiscent of the CKM constraints in the $\bar{\rho}$-$\bar{\eta}$ plane, has the advantage that it allows to transparently show the impact of individual observables on the constraints. A similar approach has been used e.g. in [14, 15, 17] for the SM Wilson coefficients and in [12] for C_7 vs. C_7'. Moreover, in some cases a pair of Wilson coefficients (or a single complex coefficient) captures already the dominant NP effect in certain scenarios, in which case such plots become particularly useful. For example, in the MSSM with MFV and flavour blind phases [81], in effective SUSY with flavour blind phases [82] and in effective SUSY with a U(2)^3 symmetry [83, 84], NP effects in $\Delta B = \Delta S = 1$ processes arise almost exclusively through complex contributions to C_7 (and C_8). In MFV models with dominance of Z penguins and without new sources of CP violation, only the real parts of C_7 and C_{10} are relevant as will be discussed in section 4.

The resulting plots are shown in figure 2. In these plots, the dark and light red regions show the 1 and 2σ best fit regions (contours of $\chi^2_{\rm tot} - \chi^2_{\rm tot,min} = 1$ or 4), while the shaded regions in different colours show the 2σ allowed regions (contours of $\chi^2 - \chi^2_{\rm min} = 4$) from $B \to K^* \mu^+ \mu^-$ at low q^2 (blue), $B \to K^* \mu^+ \mu^-$ at high q^2 (green), $B \to X_s \ell^+ \ell^-$ (brown), BR($B \to X_s \gamma$) (yellow) and $B \to K^* \gamma$ (purple). We only show the observables that give relevant constraints.

We make several observations.

- At the 95% C.L., all best fit regions are compatible with the SM.

- In the complex C_7 plane, which is relevant e.g. for the models with flavour blind phases mentioned above, the inclusive and exclusive $b \to s \ell^+ \ell^-$ observables — in particular the measurement of BR($B \to X_s \ell^+ \ell^-$) at low q^2 [13] and the LHCb measurement of $A_{\rm FB}$ at low q^2 — exclude a sign-flip in the low-energy $C_7^{\rm eff}$ that would be allowed by BR($B \to X_s \gamma$) and that was favoured by Belle data on $A_{\rm FB}$ [58]. We observe that an imaginary part of C_7 as large as $|{\rm Im}(C_7)| \lesssim 0.7$ is still allowed in this scenario.

- In the presence of C_7', the current data on the time-dependent CP asymmetry in $B \to K^* \gamma$ gives already an important constraint.

- Similar to the complex C_7 plane, in the ${\rm Re}(C_7)$–${\rm Re}(C_7')$ plane a sign-flip in $C_7^{\rm eff}$ is excluded by the inclusive and exclusive $b \to s \ell^+ \ell^-$ observables. Imposing also the constraint from $S_{K^* \gamma}$ leaves only two disjoint regions at 95% C.L.: one around the SM point and a second, less favoured one with a large ${\rm Re}(C_7') \simeq 0.5$.

- In the complex C_9 and C_{10} planes, sign flips of the real parts are excluded but imaginary parts as large as $|{\rm Im}(C_9)|, |{\rm Im}(C_{10})| \lesssim 3$ are still allowed.

- The slight preference towards non-SM values of the Wilson coefficients in the complex C_9' and C_{10}' planes results from the tension between SM prediction and experimental data on BR($B \to X_s \ell^+ \ell^-$) in the high q^2 region as well as the tension between SM
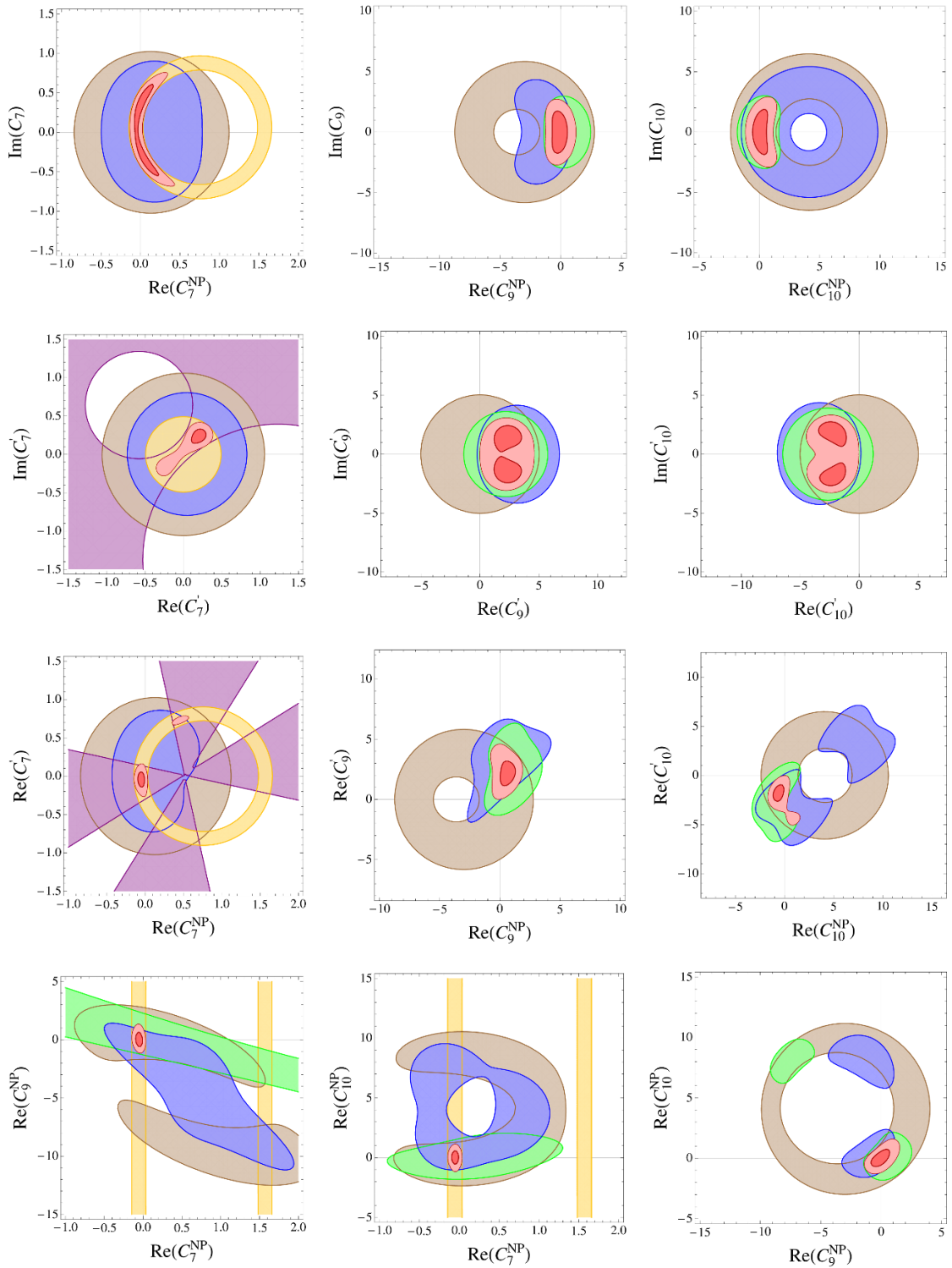
Figure 2. Individual 2σ constraints on pairs of Wilson coefficients from $B \to K^* \mu^+ \mu^-$ at low q^2 (blue) and high q^2 (green), $B \to X_s \ell^+ \ell^-$ (brown), $\mathrm{BR}(B \to X_s \gamma)$ (yellow), $B \to K^* \gamma$ (purple) and combined 1 and 2σ constraints (red).

and experimental data on F_L in $B \to K^* \mu^+ \mu^-$ at low q^2. The tension in F_L is also the reason for the slight preference for a non-SM value in the complex C_7' plane.

- High-q^2 data on $B \to K^* \ell^+ \ell^-$ are competitive with and coplementary to the low-q^2 ones. In particular, they are crucial to exclude a sign flip in $\mathrm{Re}(C_{10})$ as well as simultaneous sign flips in C_{10} and C_{10}' or C_7 and C_9.

- In the $\mathrm{Re}(C_9)$–$\mathrm{Re}(C_{10})$ plane, a simultaneous sign flip in C_9 and C_{10} would be allowed by high q^2 data on $B \to K^* \ell^+ \ell^-$ but is excluded by the new A_{FB} measurement at low q^2 from LHCb.

We stress that the above conclusions hold if one allows only the two quantities shown to be non-zero. In many NP models, several of the Wilson coefficients will deviate from the SM, which renders some or all of these constraints ineffective. The more general case calls for a *global* fit of all Wilson coefficients.

3.2 Global fit of Wilson coefficients

While the constraints discussed above are useful to display the constraining power of individual observables, they are not suited to put constraints on Wilson coefficients in models where more than two real or more than one complex coefficient is relevant, since cancellations can easily occur that render some of the constraints ineffective. Therefore, we now present constraints on Wilson coefficients varying not only 2 but all (or a subset) of the 6 complex coefficients $C_{7,9,10}^{(\prime)}$. To cope with the large dimensionality of the parameter space, we perform a Markov Chain Monte Carlo (MCMC) analysis. Details on the statistical approach are given in appendix A.

In concrete NP models, the contributions to the 6 Wilson coefficients $C_{7,9,10}^{(\prime)}$ are typically highly correlated and not all of them receive NP contributions. In addition to a completely generic case, we will therefore consider several restricted scenarios, that are each representative for a vast class of models:

1. *Real left-handed currents*, $C_i \in \mathbb{R}$, $C_i' = 0$. This is realised e.g. in models with MFV in the definition of [1, 2], i.e. no CP violation beyond the CKM phase.

2. *Complex left-handed currents*, $C_i \in \mathbb{C}$, $C_i' = 0$. This is realised e.g. in models with MFV and flavour-blind phases.

3. *Complex right-handed currents*, $C_i' \in \mathbb{C}$, $C_i = 0$.

4. *Generic NP*, $C_i \in \mathbb{C}$, $C_i' \in \mathbb{C}$.

We remark that the results of the MFV setup analysed in [11] are recovered as a limiting case of our scenario 1 when the flavour mixing angles are taken to be CKM-like.[7]

---

[7]In principle, in MFV, we should also account for the constraints arising from $b \to d$ and $s \to d$ transitions, such as $\mathrm{BR}(K_L \to \mu^+ \mu^-)$, $\mathrm{BR}(K \to \pi \ell^+ \ell^-)$ or $\mathrm{BR}(B \to X_d \gamma)$ [85]. In practise, the latter turn out to be less stringent compared to the constraints from $b \to s$ transitions.
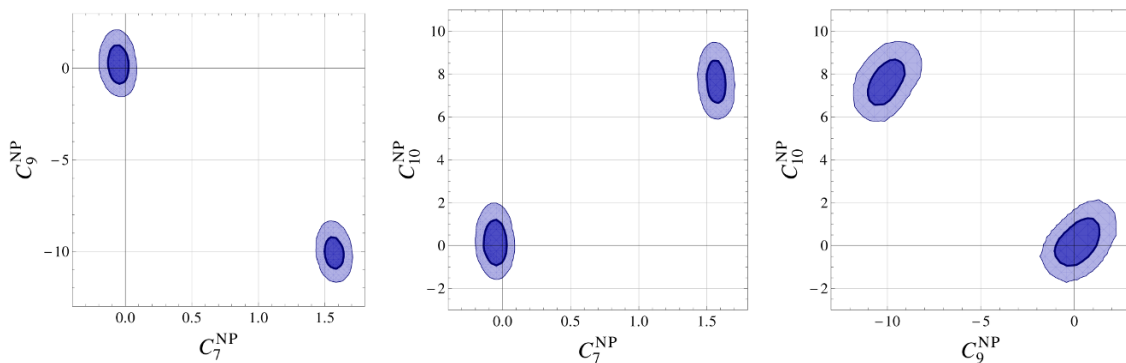
Figure 3. Constraints between Wilson coefficients in the scenario with real left-handed currents. Shown are 68% and 95% C.L. regions.

3.2.1 Real left-handed currents

In this scenario, there are only 3 free parameters, the real Wilson coefficients $C_{7,9,10}$. Figure 3 shows the 68% and 95% confidence regions in the planes of two Wilson coefficients.[8] While departures from the SM point are already quite strongly restricted, a crucial feature is the presence of a second allowed region, characterised by a simultaneous sign flip of C_{10} as well as of the effective low-energy coefficients C_7^{eff} and C_9^{eff}. A sign flip of only C_9^{eff} and C_7^{eff} or C_{10} and C_7^{eff} is excluded mainly by high-q^2 $B \to K^* \mu^+ \mu^-$ data, as was discussed already in [14]. Interestingly, a sign flip of only C_9^{eff} and C_{10} is now excluded as well by the precise A_{FB} measurement at low q^2 (see section 3.1). We remark that an overall sign flip of all Wilson coefficients cannot be excluded by low-energy data alone, since all observables involve squared amplitudes or interference terms, which are invariant under such a sign flip. On the other hand, a NP model which generates effects in C_7, C_9 and C_{10} which are each twice as large as their SM contributions seems highly unlikely. In the region with SM-like signs, we obtain the constraints

$$C_7^{\text{NP}} \in [-0.15, 0.03] \,, \qquad C_9^{\text{NP}} \in [-1.1, 1.6] \,, \qquad C_{10}^{\text{NP}} \in [-1.2, 1.6] \,, \tag{3.2}$$

at 95% C.L. These constraints can be translated into bounds on an effective NP scale Λ that suppresses NP contributions to the corresponding higher dimensional operators in the effective Hamiltonian

$$\mathcal{H}_{\text{eff}}^{\text{NP}} = \frac{c_7^{bs}}{\Lambda_7^2} \mathcal{O}_7 + \frac{c_9^{bs}}{\Lambda_9^2} \mathcal{O}_9 + \frac{c_{10}^{bs}}{\Lambda_{10}^2} \mathcal{O}_{10} \quad + \text{h.c.} \, . \tag{3.3}$$

Assuming the coefficients c_i^{bs} to be 1, and using 95% C.L. bounds on the absolute values of the Wilson coefficients we obtain

$$\Lambda_7 > 55 \text{ TeV} \,, \quad \Lambda_9 > 20 \text{ TeV} \,, \quad \Lambda_{10} > 21 \text{ TeV} \, . \tag{3.4}$$

These bounds on the effective NP scale are still weaker than the ones that can be obtained from considering dimension 6 operators that contribute to B_s mixing [86].

---

[8]Here and in the following, by "C.L." we mean Bayesian confidence regions, i.e. regions containing 68% or 95% of the Markov chain points.
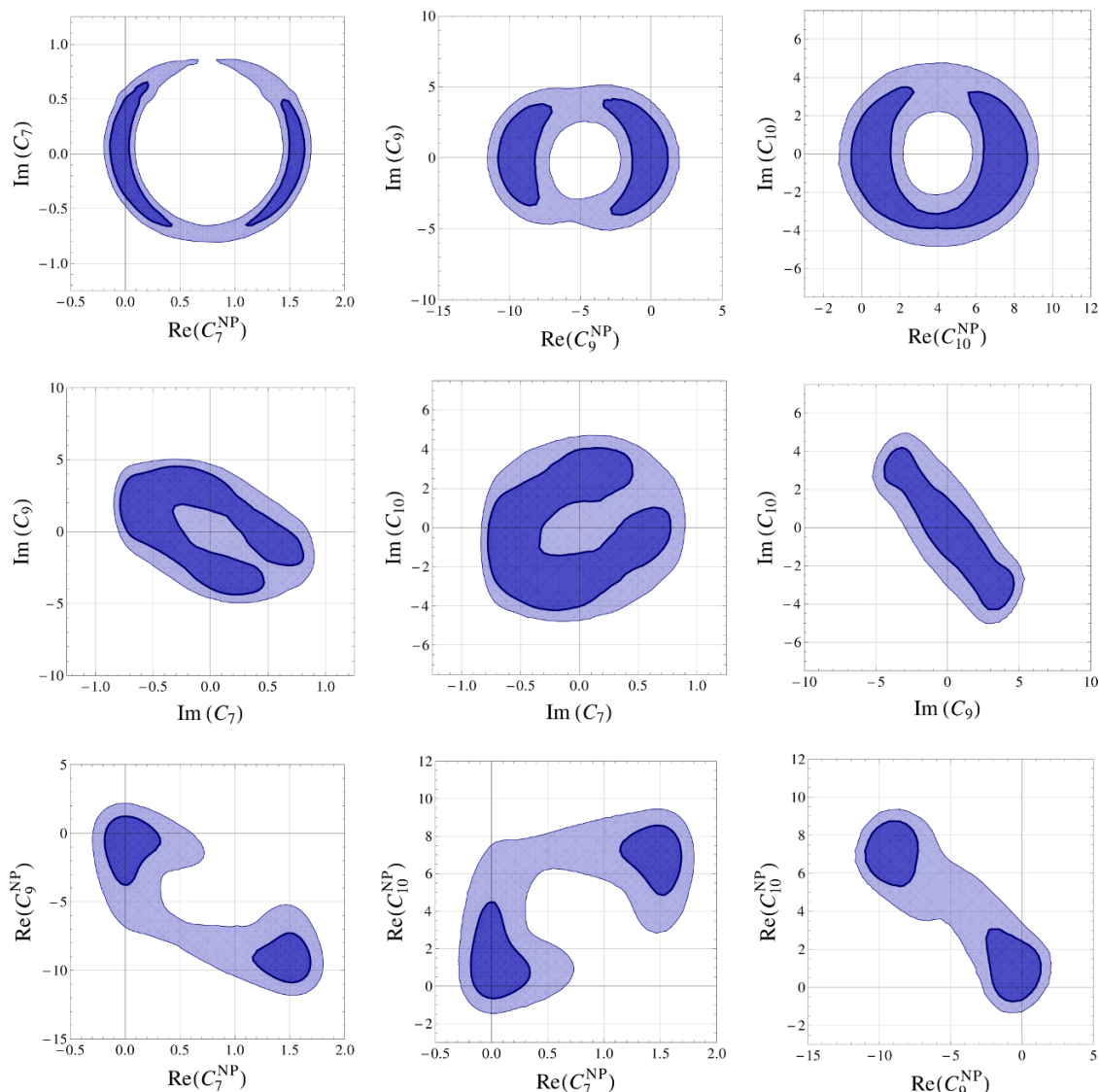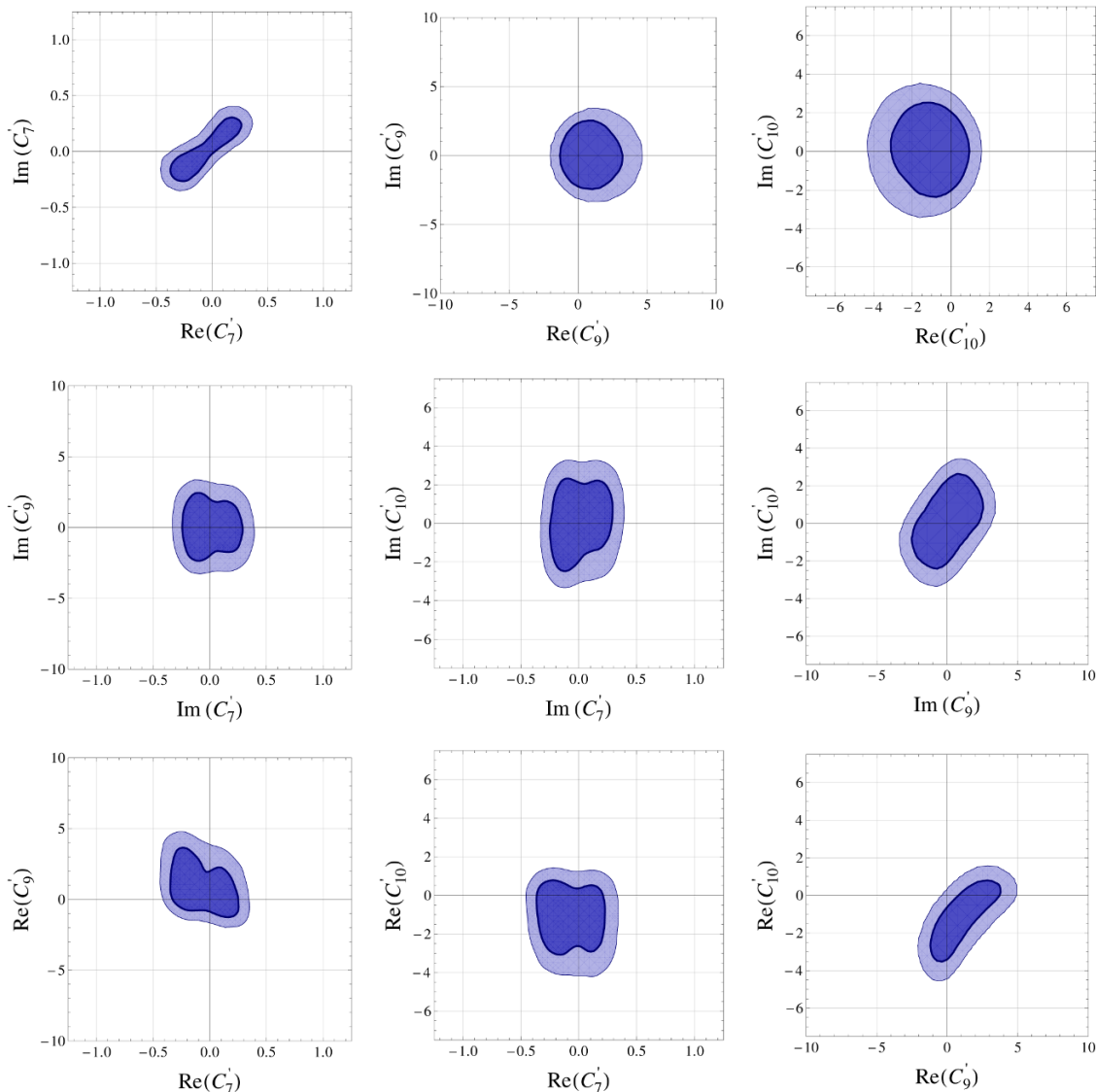
Figure 4. Constraints between Wilson coefficients in the scenario with complex left-handed currents. Shown are 68% and 95% C.L. regions.

3.2.2 Complex left-handed currents

Complex contributions to the Wilson coefficients $C_{7,9,10}$ with vanishing C'_i are predicted e.g. in models with MFV and flavour-blind phases. Figure 4 shows the 68% and 95% confidence regions in the planes of two Wilson coefficients, omitting plots lacking a correlation. At 68% C.L., we observe two solutions for the real parts of the Wilson coefficients, corresponding to a SM-like case and a case with a simultaneous sign flip in the low-energy values of C_{10}, C_7^{eff} and C_9^{eff}. However, the room for NP is much larger than in the case without non-standard CP violation since the increased number of free parameters allows for compensations among different contributions. In particular, sizable imaginary parts are allowed for all three coefficients and this implies, in turn, potentially large effects in CP
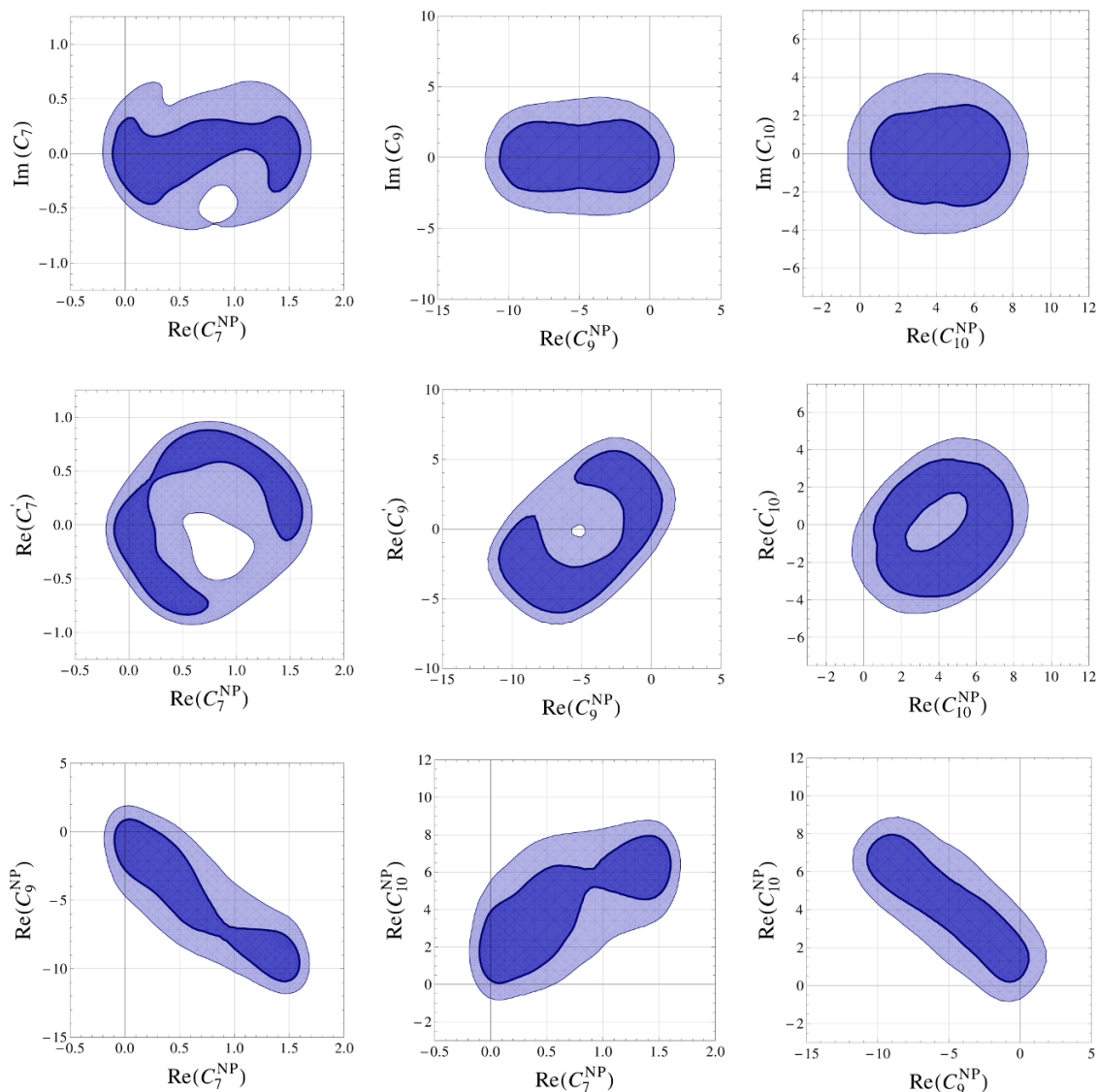
Figure 5. Constraints between Wilson coefficients in the scenario with complex right-handed currents. Shown are 68% and 95% C.L. regions.

violating observables, as will be quantified in section 3.2.6. A strong anti-correlation can be observed between the imaginary parts of C_9 and C_{10}, driven mostly by the forward-backward asymmetry in $B \to K^* \mu^+ \mu^-$ at high q^2.

3.2.3 Complex right-handed currents

Figure 5 shows the 68% and 95% confidence regions in the planes of two Wilson coefficients, omitting plots lacking a correlation. One of the most prominent differences we can observe compared to the case of left-handed currents, is the absence of two solutions for the real and imaginary parts of the Wilson coefficients. This can be mainly traced back to the lack of interference between right-handed currents with the SM contributions in inclusive decays, which forbids sign flips in the low-energy values of the Wilson coefficients. Also in this

Figure 6. Constraints between Wilson coefficients in the case of generic NP. Shown are 68% and 95% C.L. regions.

scenario the NP room for the imaginary parts of C'_7, C'_9 and C'_{10} is quite sizable and this will induce large effects in CP violating observables, as discussed in section 3.2.6. However, some of the correlations among low energy observables turn out to be different compared to the case of left-handed current, providing a tool to distinguish the two scenarios.

3.2.4 Generic NP

In this fit, we allowed all six Wilson coefficients $C^{(\prime)}_{7,9,10}$ to assume arbitrary complex values. Figure 6 shows the 68% and 95% confidence regions in the planes of two Wilson coefficients, omitting plots lacking a correlation. Sizable effects are not ruled out in any of the Wilson coefficients. However, some observations can be made, which are, by means of the generality of this fit, valid *for any theory* beyond the SM.

- For C_7, C_9 and C_{10} there is little room left for constructive interference of real NP contributions with the SM. Concretely, we find at 95% C.L.

$$\operatorname{Re} C_7^{\mathrm{NP}} > -0.01\,, \qquad \operatorname{Re} C_9^{\mathrm{NP}} < 0.2\,, \qquad \operatorname{Re} C_{10}^{\mathrm{NP}} > 0.5\,. \qquad (3.5)$$

  The slight preference for non-standard C_{10} is again driven by the tension between SM and experiment in $\mathrm{BR}(B \to X_s \ell^+ \ell^-)$ at high q^2 and $F_L(B \to K^* \mu^+ \mu^-)$ at low q^2.

- A sizable negative real NP contribution to C_9 requires comparably large (with respect to the SM) *positive* contributions to C_{10} and C_7.

- Large imaginary parts for all coefficients and large chirality-flipped coefficients are still allowed.

The last point highlights the importance of measuring observables sensitive to right-handed currents and to CP violation, such as the $B \to K^* \mu^+ \mu^-$ observables $A_{7,8,9}$ and S_3.

3.2.5   Predictions for $B_s \to \mu^+ \mu^-$ and $B_s \to \tau^+ \tau^-$

Due to its sensitivity to scalar currents, we did not include the branching ratios of $B_s \to \mu^+ \mu^-$ and $B_s \to \tau^+ \tau^-$ in our fits. Instead, using the constraints on $C_{10}^{(\prime)}$, we can now give upper limits on the branching ratios in the considered scenarios assuming the scalar and pseudoscalar Wilson coefficients to be negligible. These bounds are useful since an observed violation of them would imply the presence of scalar currents. The values we find at 95% C.L. are listed in table 3. In the scenario with right-handed currents as well as in the case of generic NP, a significant suppression of the branching ratios is possible. The upper bounds on $\mathrm{BR}(B_s \to \mu^+ \mu^-)$ in all cases are approximately a factor of 2 below the current experimental bound (2.4) and correspond roughly to a 50% enhancement of the branching ratio with respect to the SM. Due to the new measurement of $B \to K^* \mu^+ \mu^-$ angular observables, they are stronger than similar bounds presented in the literature before [14].

We stress that scalar current effects in $B_s \to \mu^+ \mu^-$ could still enhance the branching ratio over its current experimental bound.

Let us also mention that in the case of $B_d \to \mu^+ \mu^-$, both the effects induced by the corresponding $b \to d$ Wilson coefficient $C_{10}^{(\prime)}$ and scalar currents can enhance the branching ratio of $B_d \to \mu^+ \mu^-$ over the experimental bound since the corresponding constraints from $b \to d \ell^+ \ell^-$ processes are weaker. In addition, we remark that the ratio $\mathrm{BR}(B_d \to \mu^+ \mu^-)/\mathrm{BR}(B_s \to \mu^+ \mu^-)$ can significantly depart from the SM as well as the MFV predictions $\mathrm{BR}(B_d \to \mu^+ \mu^-)/\mathrm{BR}(B_s \to \mu^+ \mu^-) \approx |V_{td}/V_{ts}|^2$ in both directions.

Finally, we discuss the allowed values for the branching ratio of $B_s \to \tau^+ \tau^-$. From the general expressions of $\mathrm{BR}(B_s \to \ell^+ \ell^-)$ in presence of NP (see eq. (2.5)) one has

$$\frac{\mathrm{BR}(B_s \to \tau^+ \tau^-)}{\mathrm{BR}(B_s \to \mu^+ \mu^-)} \simeq \left(1 - \frac{4m_\tau^2}{m_{B_s}^2}\right)^{1/2} \frac{m_\tau^2}{m_\mu^2} \times \frac{\left(1 - 4m_\tau^2/m_{B_s}^2\right) |S|^2 + |P|^2}{|S|^2 + |P|^2}\,, \qquad (3.6)$$

where S and P have been defined in eq. (2.6).

Scenario	BR($B_s \to \mu^+\mu^-$)	BR($B_s \to \tau^+\tau^-$)	$|\langle A_7 \rangle_{[1,6]}|$	$|\langle A_8 \rangle_{[1,6]}|$	$|\langle A_9 \rangle_{[1,6]}|$	$\langle S_3 \rangle_{[1,6]}$
Real LH	$[1.0, 5.6] \times 10^{-9}$	$[2, 12] \times 10^{-7}$	0	0	0	0
Complex LH	$[1.0, 5.4] \times 10^{-9}$	$[2, 12] \times 10^{-7}$	< 0.31	< 0.15	0	0
Complex RH	$< 5.6 \times 10^{-9}$	$< 12 \times 10^{-7}$	< 0.22	< 0.17	< 0.12	$[-0.06, 0.15]$
Generic NP	$< 5.5 \times 10^{-9}$	$< 12 \times 10^{-7}$	< 0.34	< 0.20	< 0.15	$[-0.11, 0.18]$
LH Z peng.	$[1.4, 5.5] \times 10^{-9}$	$[3, 12] \times 10^{-7}$	< 0.27	< 0.14	0	0
RH Z peng.	$< 3.8 \times 10^{-9}$	$< 8 \times 10^{-7}$	< 0.22	< 0.18	< 0.12	$[-0.03, 0.18]$
Generic Z p.	$< 4.1 \times 10^{-9}$	$< 9 \times 10^{-7}$	< 0.28	< 0.21	< 0.13	$[-0.07, 0.19]$
scalar current	$< 1.1 \times 10^{-8}$	$< 1.3(2.3) \times 10^{-6}$	0	0	0	0

Table 3. Predictions at 95% C.L. for the branching ratios of $B_s \to \mu^+\mu^-$ and $B_s \to \tau^+\tau^-$ and predictions for low-q^2 angular observables in $B \to K^*\mu^+\mu^-$ (neglecting tiny SM effects below the percent level) in all the scenarios. The scenarios "Real LH", "Complex LH", "Complex RH", "Generic NP", "LH Z peng.", "RH Z peng.", and "Generic Z p." correspond to the scenarios discussed in section 3.2.1, section 3.2.2, section 3.2.3, section 3.2.4, section 4.1.1, section 4.1.2, and section 4.1.3, respectively, assuming negligible (pseudo)scalar currents. In the scenario "scalar current" *only* scalar currents are considered. The number quoted for $B_s \to \tau^+\tau^-$ in the "scalar current" scenario refers to the maximum value for its branching ratio in the case of dominant scalar (pseudoscalar) currents.

In the case where $C_{10}^{(\prime)}$ provides the dominant NP effects, one obtains

$$\frac{\text{BR}(B_s \to \tau^+\tau^-)}{\text{BR}(B_s \to \mu^+\mu^-)} \simeq 212 \,, \tag{3.7}$$

which implies, in particular, the SM prediction for the branching ratio of $B_s \to \tau^+\tau^-$

$$\text{BR}(B_s \to \tau^+\tau^-)_{\text{SM}} = (7.7 \pm 0.8) \times 10^{-7} \,. \tag{3.8}$$

In the case where (pseudo)scalar current effects dominate, $\text{BR}(B_s \to \mu^+\mu^-)$ can saturate the current experimental bound while for $\text{BR}(B_s \to \tau^+\tau^-)$ we get

$$120 \lesssim \frac{\text{BR}(B_s \to \tau^+\tau^-)}{\text{BR}(B_s \to \mu^+\mu^-)} \lesssim 212 \,, \tag{3.9}$$

where the lower (upper) bound in eq. (3.9) correspond to the case where the scalar (pseudoscalar) contribution dominates.

Combining eq. (2.3) with eq. (3.9), it turns out that $\text{BR}(B_s \to \tau^+\tau^-) \lesssim 2 \times 10^{-6}$ (see also table 3) and it has to be seen whether such values might be within the reach of LHCb. However, we stress that this upper bound relies on the assumption that the (pseudo)scalar Wilson coefficients $C_{S,P}^{(\prime)}$ are linearly proportional to the lepton Yukawa couplings, as discussed in section 2. If we relax this assumption, as it might be the case in models like R-parity violating SUSY [87] or models with enhanced couplings with the third lepton generation (compared to the linear scaling assumed throughout this work), $\text{BR}(B_s \to \tau^+\tau^-)$ could get in principle much larger values than 10^{-6}.
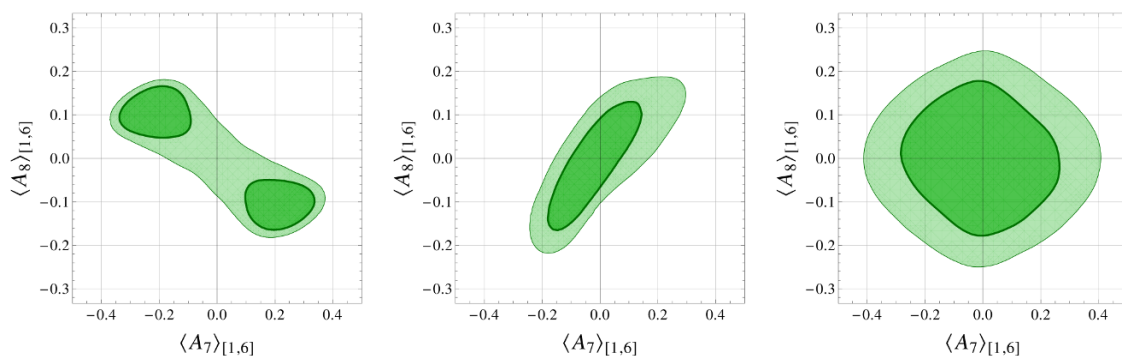
Figure 7. Fit predictions for the low-q^2 CP asymmetries $\langle A_{7,8} \rangle$ in $B \to K^* \mu^+ \mu^-$ in the case of complex left-handed currents (left), complex right-handed currents (centre) and generic NP (right). Shown are 68% and 95% C.L. regions.

3.2.6 Predictions for $B \to K^* \mu^+ \mu^-$

Figure 7 shows the predictions for the T-odd $B \to K^* \mu^+ \mu^-$ CP asymmetries A_7 and A_8 at low q^2 for the scenarios with complex left-handed currents, complex right-handed currents and for generic NP. In the absence of right-handed currents, one finds an anti-correlation between A_7 and A_8 which has already been found in models where only C_7 contributes [55, 82, 84] (see also [88]), but is shown here to hold under more general conditions. At 68% C.L., one finds a preference for non-standard CP asymmetries driven mostly by the tension between SM and experiment in $F_L(B \to K^* \mu^+ \mu^-)$ at low q^2. Similarly, in the absence of complex left-handed currents, one finds an opposite correlation. In the generic case, there is no correlation at all. Interestingly, in all three scenarios, large effects in both asymmetries are still allowed, with the numerical bounds listed in table 3. Future measurements of A_7 and A_8 at LHCb will thus be crucial to constrain the imaginary parts of the Wilson coefficients entering the $B \to K^* \mu^+ \mu^-$ decay.

Also shown in table 3 are the predictions for the CP asymmetry A_9 and the CP-averaged angular coefficient S_3 at low q^2, both of which are tiny in the SM but can be sizable in presence of right-handed currents. Indeed, both observables can assume values in excess of 10% in the complex right-handed scenario and for generic NP.

We note that the CDF measurement of S_3 and A_9 shown in the last two rows of table 2 currently puts no significant constraints on NP, yet. Future measurements at LHCb with errors of the order of 0.1 will however put important constraints on CP-violating or CP-conserving right-handed currents.

4 Analysis of flavour-changing Z couplings

Tree level FCNC couplings of the Z boson can appear in a number of NP scenarios. Prominent examples are the SM with four non-sequential generations of quarks and models with an extra U(1) symmetry [89, 90]. Moreover, the contributions to the semi-leptonic operators

are dominated by Z penguins, i.e. loop-induced modified Z couplings,[9] in many theories, e.g. in the MSSM [92, 94]. It is therefore interesting to consider the effects in a framework with modified $\bar{s}bZ$ couplings, which can be parametrised by the effective Lagrangian [92]

$$\mathcal{L}_{\text{eff}}^{\bar{s}bZ} = -\frac{G_F}{\sqrt{2}}\frac{e}{\pi^2}m_Z^2 c_w s_w V_{tb}^* V_{ts}\, Z^\mu\, (Z_L\, \bar{s}\gamma_\mu P_L b + Z_R\, \bar{s}\gamma_\mu P_R b)\,, \tag{4.1}$$

with $s_w = \sin\theta_w$ and $c_w = \cos\theta_w$. In this class of models one finds

$$C_{10}^{\text{NP}} = Z_L^{\text{NP}}\,, \qquad\qquad C_{10}' = Z_R\,, \tag{4.2}$$
$$C_9^{\text{NP}} = -Z_L^{\text{NP}}(1 - 4s_w^2)\,, \qquad\qquad C_9' = -Z_R(1 - 4s_w^2)\,. \tag{4.3}$$

The contributions to $C_9^{(\prime)}$ are strongly suppressed by the small vector coupling of the Z to charged leptons $(1 - 4s_w^2) \approx 0.08$.

The modified $\bar{b}sZ$ couplings also modify decays with a neutrino pair in the final state, so one obtains correlations between $b \to s\nu\bar{\nu}$ and $b \to s\ell^+\ell^-$ observables. Writing the $b \to s\nu\bar{\nu}$ effective Hamiltonian as

$$\mathcal{H}_{\text{eff}} = -\frac{4\,G_F}{\sqrt{2}}V_{tb}V_{ts}^*(C_L\mathcal{O}_L + C_R\mathcal{O}_R)\ +\ \text{h.c.}\,, \tag{4.4}$$

$$\mathcal{O}_{L,R} = \frac{e^2}{8\pi^2}(\bar{s}\gamma_\mu P_{L,R}b)(\bar{\nu}\gamma^\mu P_L\nu)\,, \tag{4.5}$$

The effective Lagrangian (4.1) leads to

$$C_L = C_L^{\text{SM}} + Z_L^{\text{NP}}\,, \qquad C_R = Z_R\,, \tag{4.6}$$

where $C_L^{\text{SM}} = -6.38 \pm 0.06$ [93].

Finally, an effective tree level contribution to B_s-$\bar{B}_s$ mixing is generated by the exchange of a Z with modified $\bar{b}sZ$ coupling. Its contribution to the mixing amplitude can be written at the scale m_Z as [93]

$$\frac{\langle B_s|\mathcal{H}|\bar{B}_s\rangle^{\bar{s}bZ}}{\langle B_s|\mathcal{H}|\bar{B}_s\rangle^{\text{SM}}} = \frac{4\alpha s_w^2}{\pi S_0(x_t)}(Z_L^2 - 3.5\,Z_L Z_R + Z_R^2)\,. \tag{4.7}$$

We consider three scenarios in the following:

- *Left-handed modified Z couplings*, $Z_L \in \mathbb{C}$, $C_7^{\text{NP}} \in \mathbb{C}$, $Z_R = C_7' = 0$,

- *Right-handed modified Z couplings*, $Z_R \in \mathbb{C}$, $C_7' \in \mathbb{C}$, $Z_L^{\text{NP}} = C_7^{\text{NP}} = 0$,

- *Generic modified Z couplings*, $Z_{L,R} \in \mathbb{C}$, $C_7^{(\prime)} \in \mathbb{C}$,

allowing for non-standard CP violation in all cases. The generic case covers all NP models where contributions to the semileptonic operators are dominated by Z penguins. This includes in particular the general MSSM [92, 94]. The fitting procedure is as described in section 3.2.

---

[9]We remark that the distinction between Z penguins and other contributions is in general gauge dependent. However, this gauge dependence is weak if Z penguins dominate [91–93].
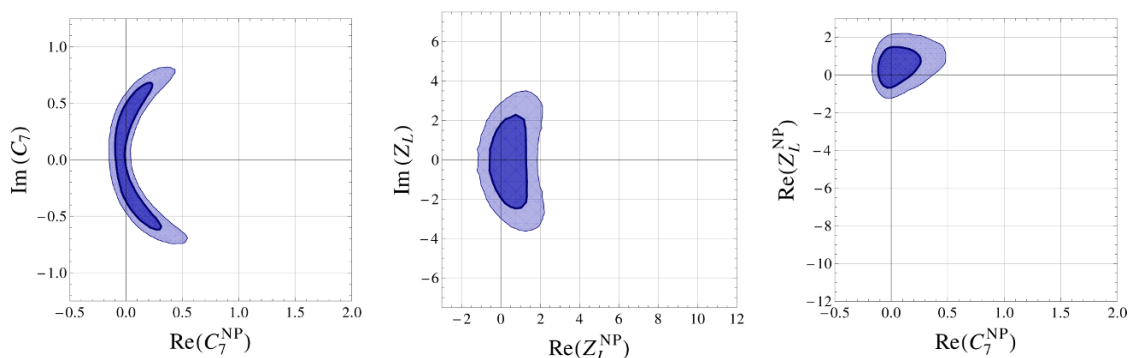
Figure 8. Constraints on C_7 and the modified Z coupling in the scenario with left-handed couplings only. Shown are 68% and 95% C.L. regions.

4.1 Constraints on modified Z couplings

4.1.1 Left-handed modified Z couplings

Figure 8 shows the 68% and 95% confidence regions in the complex planes of C_7 and Z_L as well as the correlation between the real parts of C_7 and Z_L. The constraint in the C_7 plane is basically identical to the constraint in the absence of semileptonic operators shown in the upper left plot of figure 2, which is in contrast to the corresponding constraint in the presence of C_9 and C_{10} shown in figure 4, where large effects in $\mathrm{Re}(C_7)$ (and in particular a sign flip) were allowed. This can be traced back to the suppression of C_9 compared to C_{10} in the Z penguin scenario, making impossible a simultaneous sign flip of C_7^{eff} and C_9^{eff} at low energies, which would be required in particular to meet the constraint from $A_{\mathrm{FB}}(B \to K^* \mu^+ \mu^-)$ at low q^2. For the same reason, the correlation of the real parts of C_7 and Z_L only shows one solution.
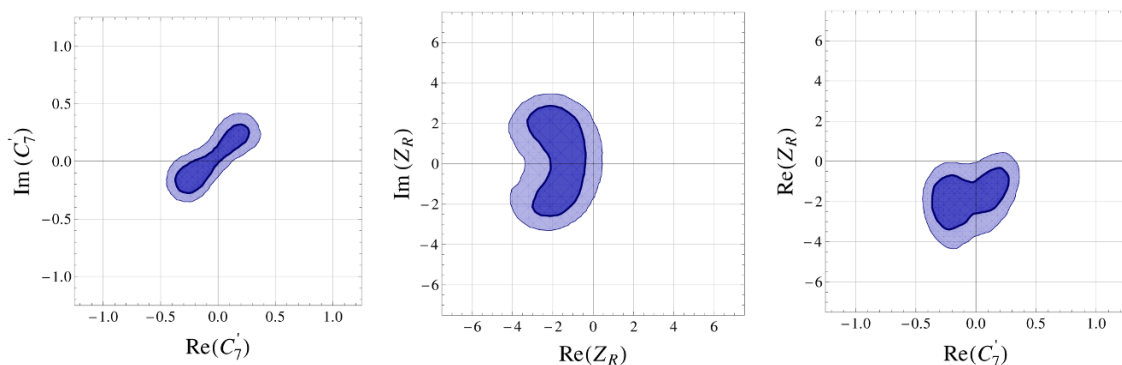
4.1.2 Right-handed modified Z couplings

Figure 9 shows the 68% and 95% confidence regions in the complex planes of C_7' and Z_R as well as the correlation between the real parts of C_7' and Z_R. The constraint in the C_7' plane is very similar to the constraint in the absence of semileptonic operators shown in the corresponding plot of figure 2. The negative values preferred for the real part of the right-handed Z coupling, i.e. for $\mathrm{Re}(C_{10}')$, arises from low- and high q^2 $B \to K^* \mu^+ \mu^-$ data, as can be seen in the corresponding plot of figure 2.
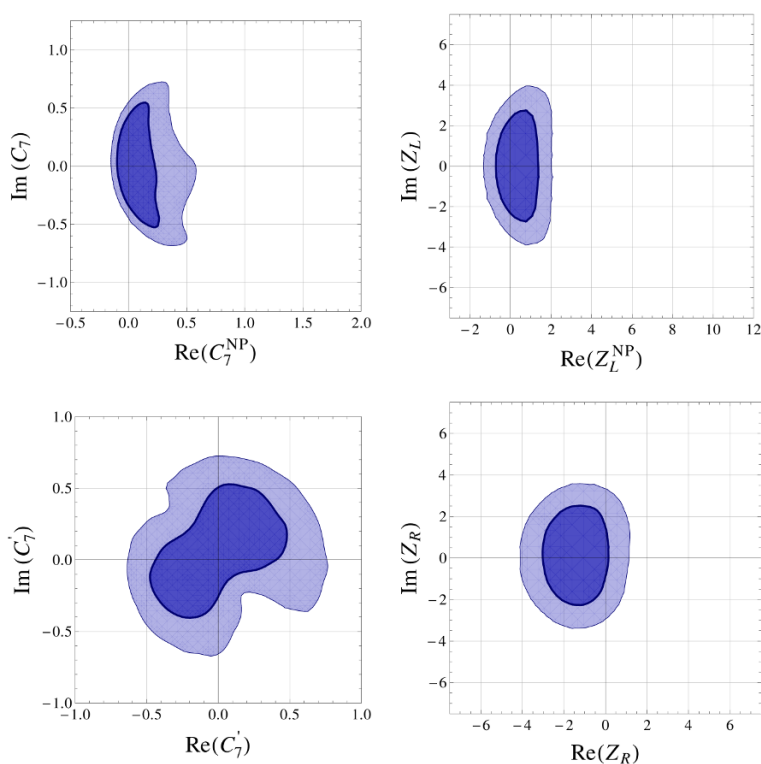
4.1.3 Generic modified Z couplings

Figure 10 shows the 68% and 95% confidence regions in the complex planes of the Wilson coefficients $C_7^{(\prime)}$ and the couplings $Z_{L,R}$ in the case of generic modified Z penguins. While the room for NP is larger than in the more constrained previous cases, also in the generic there are no disjoint solutions for the Wilson coefficients. We are thus lead to conclude on a model-independent basis that if the NP contributions to semi-leptonic operators are dominated by Z penguins, the real parts of the Wilson coefficients $C_{7,9,10}$ at low energies must have the same sign as in the SM.

Figure 9. Constraints on C_7 and the modified Z coupling in the scenario with right-handed couplings only. Shown are 68% and 95% C.L. regions.


Figure 10. Constraints on $C_7^{(\prime)}$ and the modified Z couplings in the scenario with generic modified Z couplings. Shown are 68% and 95% C.L. regions.

4.2 Fit predictions

4.2.1 Predictions for $B_s \to \mu^+\mu^-$, $B_s \to \tau^+\tau^-$ and $B \to K^*\mu^+\mu^-$

Analogously to section 3.2.5, we can give fit predictions for $\mathrm{BR}(B_s \to \mu^+\mu^-)$ and $\mathrm{BR}(B_s \to \tau^+\tau^-)$ in the absence of scalar currents and for $B \to K^*\mu^+\mu^-$ observables in the considered modified Z coupling scenarios based on the constraints obtained in the global fit. The allowed ranges are shown in table 3. In the generic case, the preference for smaller values
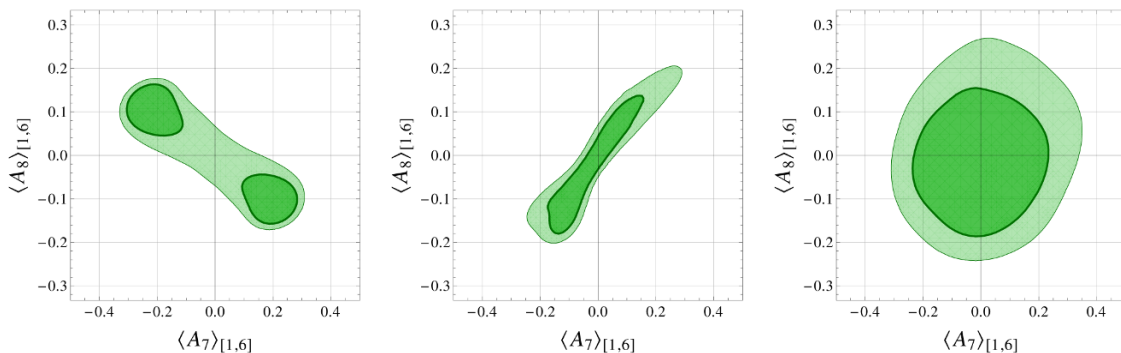
Figure 11. Fit predictions for the low-q^2 CP asymmetries $\langle A_{7,8} \rangle$ in $B \to K^* \mu^+ \mu^-$ for the scenario with left-handed (left), right-handed (centre) or generic (right) modified Z couplings. Shown are 68% and 95% C.L. regions.

of the $B_s \to \mu^+ \mu^-$ and $B_s \to \tau^+ \tau^-$ branching ratios is due to the negative values preferred for $\text{Re}(Z_R)$ (cf. section 4.1.2), i.e. for $\text{Re}(C'_{10})$, which leads to a destructive interference with the SM in the decay amplitudes, see eq. (2.6).

Figure 11 shows the prediction for the $B \to K^* \mu^+ \mu^-$ CP asymmetries A_7 and A_8 at low q^2 in all three scenarios. The predictions are similar to the corresponding ones obtained for generic $C_{9,10}^{(')}$ shown in figure 7, so the comments made there apply here as well. Also for the observables S_3 and A_9 we find predictions that are similar to the cases discussed in section 3.2.6. The results are summarised in table 3.

4.2.2 Predictions for B_s mixing

Since the real and imaginary parts of the left- and right-handed Z couplings are constrained by $b \to s \ell^+ \ell^-$ processes not to be significantly larger than the SM value of the (real) left-handed Z coupling, the Z exchange contribution to B_s mixing, which is negligible in the SM, cannot lead to sizable deviations from the SM. Concretely, in the considered scenarios we find, at 95% C.L.,

$$\text{left-handed mod. } Z \text{ couplings:} \quad |S_{\psi\phi} - S_{\psi\phi}^{\text{SM}}| < 0.008, \tag{4.8}$$

$$\text{right-handed mod. } Z \text{ couplings:} \quad |S_{\psi\phi} - S_{\psi\phi}^{\text{SM}}| < 0.014, \tag{4.9}$$

$$\text{generic mod. } Z \text{ couplings:} \quad |S_{\psi\phi} - S_{\psi\phi}^{\text{SM}}| < 0.04. \tag{4.10}$$

Such NP contributions are well within the range allowed by the measurement of the B_s mixing phase at LHCb [95].

4.2.3 Predictions for $b \to s \nu \bar{\nu}$ decays

The two exclusive $b \to s \nu \bar{\nu}$ decays, $B \to (K, K^*) \nu \bar{\nu}$, and the inclusive one $B \to X_s \nu \bar{\nu}$ give access to four observables sensitive to NP: the three branching ratios and the K^* longitudinal polarisation fraction F_L in $B \to K^* \nu \bar{\nu}$. However, the observables are not all independent since they depend on only two real combinations of the complex Wilson

coefficients C_L and C_R [93, 96, 97],

$$\epsilon = \frac{\sqrt{|C_L|^2 + |C_R|^2}}{|(C_L)^{\mathrm{SM}}|}, \qquad \eta = \frac{-\mathrm{Re}\,(C_L C_R^*)}{|C_L|^2 + |C_R|^2}\,. \tag{4.11}$$

For the central values of the hadronic parameters, one obtains[10] [93]

$$\mathrm{BR}(B \to K^* \nu\bar{\nu}) = 6.8 \times 10^{-6}\,(1 + 1.31\,\eta)\epsilon^2\,, \tag{4.12}$$

$$\mathrm{BR}(B \to K \nu\bar{\nu}) = 4.5 \times 10^{-6}\,(1 - 2\,\eta)\epsilon^2\,, \tag{4.13}$$

$$\mathrm{BR}(B \to X_s \nu\bar{\nu}) = 2.7 \times 10^{-5}\,(1 + 0.09\,\eta)\epsilon^2\,, \tag{4.14}$$

$$\langle F_L \rangle (B \to K^* \nu\bar{\nu}) = 0.54\,\frac{(1 + 2\,\eta)}{(1 + 1.31\,\eta)}\,, \tag{4.15}$$

where $\langle F_L \rangle$ refers to the ratio of the branching ratio into a longitudinal K^* over the total branching ratio. It can be extracted from the angular distribution of the $K^* \to K\pi$ decay products.

In the scenario with left-handed modified Z couplings only, one has $\eta = 0$, F_L is SM-like and all the branching ratios are merely scaled by a common factor. We obtain, at 95% C.L.,

$$\epsilon^2 = \frac{\mathrm{BR}(B \to K^* \nu\bar{\nu})}{\mathrm{BR}(B \to K^* \nu\bar{\nu})_{\mathrm{SM}}} = \frac{\mathrm{BR}(B \to K \nu\bar{\nu})}{\mathrm{BR}(B \to K \nu\bar{\nu})_{\mathrm{SM}}} \in [0.5, 1.3]\,. \tag{4.16}$$

In the scenario with right-handed modified Z couplings and SM-like left-handed couplings, one finds an anticorrelation between the two experimentally most promising modes, $B \to K\nu\bar{\nu}$ and $B \to K^*\nu\bar{\nu}$ (see [88, 100]). At 95% C.L., we find

$$\frac{\mathrm{BR}(B \to K^* \nu\bar{\nu})}{\mathrm{BR}(B \to K^* \nu\bar{\nu})_{\mathrm{SM}}} \in [0.6, 1.0]\,, \quad \frac{\mathrm{BR}(B \to K \nu\bar{\nu})}{\mathrm{BR}(B \to K \nu\bar{\nu})_{\mathrm{SM}}} \in [1.0, 2.6]\,, \quad \frac{\langle F_L \rangle}{\langle F_L \rangle_{\mathrm{SM}}} \in [0.4, 1.0]\,, \tag{4.17}$$

The preference for a suppression of F_L and $\mathrm{BR}(B \to K^* \nu\bar{\nu})$ but an enhancement of $\mathrm{BR}(B \to K \nu\bar{\nu})$ is again due to the negative values preferred for Z_R commented on in section 4.1.2. The large enhancement possible for $\mathrm{BR}(B \to K \nu\bar{\nu})$ is close to the current experimental bound $\mathrm{BR}(B^+ \to K^+ \nu\bar{\nu}) < 13 \times 10^{-6}$ [101].

In the case of left- *and* right-handed Z couplings, the correlation between the decays carries information on the size of left- vs. right-handed currents and is thus a valuable probe of the chirality structure of NP. In figure 12, we show the fit prediction for $B \to K\nu\bar{\nu}$ and $B \to K^*\nu\bar{\nu}$. We observe that the SM point is allowed at about 68% C.L. Also in this case, only a small enhancement or a sizable suppression is allowed for the $B \to K^*\nu\bar{\nu}$ branching ratio, while an enhancement of the $B \to K\nu\bar{\nu}$ branching ratio up to a factor of 3 is possible. For F_L, we find at 95% C.L.

$$\frac{\langle F_L \rangle}{\langle F_L \rangle_{\mathrm{SM}}} \in [0.4, 1.1]\,. \tag{4.18}$$

---

[10]A lower central value for $\mathrm{BR}(B \to K \nu\bar{\nu})$ is obtained if the experimental value of $\mathrm{BR}(B \to K \ell^+ \ell^-)$ is used, assuming the latter decay to be SM-like [98]. Here we allow both decays to deviate from the SM prediction. We treat the $B \to \tau(\to K\bar{\nu})\nu$ contribution [99] as a background to be subtracted from the experimental result.
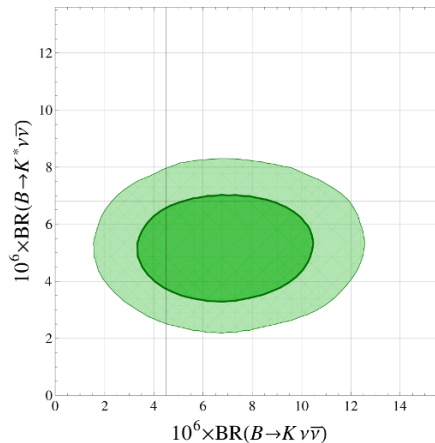
Figure 12. Fit prediction for the branching ratios of $B \to K^{(*)}\nu\bar\nu$ for generic modified Z couplings. Shown are 68% and 95% C.L. regions.

In all the scenarios, the full allowed range of branching ratios can be probed at the next-generation B factories [38].

Finally, we stress that these conclusions are only valid under the assumptions that modified Z couplings dominate the NP contributions to $b \to s\nu\bar\nu$ and $b \to s\ell^+\ell^-$ semi-leptonic operators. Much larger effects in $B \to K^{(*)}\nu\bar\nu$ are possible in models where this is not the case, e.g. models with a non-universal Z' coupling stronger to neutrinos than to charged leptons [93].

5 Conclusions

Rare decays with a $b \to s$ transition offer excellent opportunities to probe the flavour sectors of extensions of the SM. The effects of new heavy degrees of freedom in these processes can be parametrised by modifications of the Wilson coefficients of local, non-renormalizable operators, which allows to constrain such NP effects in a model-independent way. In this work, we analysed the constraints on the Wilson coefficients that follow from the currently available experimental data on $b \to s$ rare decays. We took into account the measurements from the B factories of the branching ratio of the radiative $B \to X_s\gamma$ decay, of the time-dependent CP asymmetry in $B \to K^*\gamma$, of the branching ratio of the inclusive $B \to X_s\ell^+\ell^-$ decay, Belle and CDF data on the branching ratio and angular distribution of the exclusive $B \to K^*\mu^+\mu^-$ decay and in particular the recent LHCb results on the branching ratio and angular distribution of $B \to K^*\mu^+\mu^-$.

The constraints on the Wilson coefficients are obtained by using a χ^2 function, which depends on the Wilson coefficients and contains the theory predictions for the observables and experimental averages as well as the corresponding uncertainties.

We have analysed the following scenarios where:

1. the dominant NP effects are captured already by one complex Wilson coefficient or by a pair of real Wilson coefficients. This is a representative case of many NP models like the MSSM with MFV and flavour blind phases [81, 82], non-MFV SUSY models [83, 84, 102] and also models with dominance of Z penguins;

2. the NP effects are accounted for by means of the full set of the 6 complex Wilson coefficients $C_{7,9,10}^{(\prime)}$.

3. the dominant NP effects in the semi-leptonic operators arise from non-standard flavour changing Z couplings.

While we refer to sections 3 and 4 for a detailed description of all our results, we want to emphasise here the following main messages:

- At the 95% C.L., all best fit regions are compatible with the SM.

- The combination of inclusive and exclusive $b \to s\ell^+\ell^-$ observables exclude sign flips in various low-energy WCs. That is, the SM is likely to provide the dominant effects in low energy observables. In particular, we show that

  - sign flips in C_7, C_9 or C_{10} are excluded if NP enters dominantly through Z penguins,

  - only a simultaneous sign flip of C_7, C_9 and C_{10}, which cannot be excluded by low-energy data alone, is allowed in the absence of non-standard CP violation or right-handed currents.

- The new $A_{\rm FB}$ measurement at low q^2 from LHCb is already quite effective in constraining NP effects. The same is true for the time-dependent CP asymmetry in $B \to K^*\gamma$.

- High-q^2 data on $B \to K^*\mu^+\mu^-$ are competitive with and complementary to the low-q^2 ones.

Moreover, we have investigated the implications of the above constraints and the future prospects for observables in $b \to s\ell^+\ell^-$ and $b \to s\nu\bar{\nu}$ transitions in view of improved measurements. In particular, we find that

- in the presence of non-standard CP violation, the low-q^2 angular CP asymmetries A_7 and A_8 in $B \to K^*\mu^+\mu^-$ can reach up to $\pm 35\%$ and $\pm 20\%$, respectively.

- in the presence of right-handed currents, the low-q^2 angular observables A_9 and S_3 in $B \to K^*\mu^+\mu^-$ can reach up to $\pm 15\%$.

- in the absence of (pseudo)scalar currents, $\mathrm{BR}(B_s \to \mu^+\mu^-)$ and $\mathrm{BR}(B_s \to \tau^+\tau^-)$ can be enhanced at most by 50% over their SM values, mainly due to the new measurement of $B \to K^*\mu^+\mu^-$ angular observables. In contrast, if scalar currents are at work, $\mathrm{BR}(B_s \to \mu^+\mu^-)$ can still saturate the current experimental bound and $\mathrm{BR}(B_s \to \tau^+\tau^-)$ can be enhanced by a factor of 3.

- if NP in $b \to s\ell^+\ell^-$ and $b \to s\nu\bar{\nu}$ processes is dominated by left-handed Z penguins, an enhancement of the branching ratios of $B \to K^{(*)}\nu\bar{\nu}$ by more than 30% is unlikely. If right-handed Z penguins are present, $B \to K\nu\bar{\nu}$ can saturate the present experimental bound, while $B \to K^*\nu\bar{\nu}$ is unlikely to be enhanced.

The first two points highlight the importance of measuring observables in the $B \to K^* \mu^+ \mu^-$ angular distribution sensitive to right-handed currents and CP violation. Such measurements would be crucial to lift degeneracies in the space of Wilson coefficients which make it difficult at present to put strong constraints on individual coefficients in a completely generic NP model, as our analysis in sections 3.2.2 and 3.2.4 showed.

In conclusion, the present work updates and generalises previous studies providing, at the same time, a useful tool to test the flavour structure of any theory beyond the SM.

Acknowledgments

A Statistical method

Here we give some details on our statistical method used to obtain the constraints on the Wilson coefficients in section 3.2 and 4. We use a Bayesian approach with the likelihood function

$$L(\vec{C}) = e^{-\chi^2(\vec{C})/2} \,, \tag{A.1}$$

where $\vec{C}$ is a 12-dimensional vector containing the real and imaginary parts of the 6 Wilson coefficients $C_{7,9,10}^{(\prime)}$ and the χ^2 function has been defined at the beginning of section 3. We sample the posterior probability distribution, defined according to Bayes' theorem,

$$P(\vec{C}) = \frac{L(\vec{C}) \, \pi(\vec{C})}{\int L(\vec{C}\prime) \, \pi(\vec{C}\prime) \, d\vec{C}\prime} \,, \tag{A.2}$$

by means of a Markov Chain Monte Carlo (MCMC) analysis using the Metropolis-Hastings algorithm (see e.g. the review on statistics in [103]). As proposal density, we use a multivariate Gaussian, whose width is optimised to tune the acceptance rate. We use a flat prior, $\pi(\vec{C}) = 1$, in the general case and a multivariate δ function in the restricted scenarios. The stationary density distribution of points in the Markov chain is proportional to $P(\vec{C})$. Constraints on two-dimensional subspaces are obtained by projecting the points onto this plane. Predictions for observables presented in sections 3.2 and 4 are obtained by evaluating the observable for central values of the theoretical input parameters at each point in the chain and interpreting their density distribution as posterior probability for the observable.

Two-dimensional confidence regions in sections 3.2 and 4 are obtained by determining contours of constant posterior probability which contain 68% (or 95%) of the Markov chain points. Analogously, one-dimensional confidence regions are highest posterior density intervals, i.e. the posterior probability is higher everywhere inside the interval than outside, and they contain 68% (or 95%) of the points.

B Effective Wilson coefficients

In sections 3 and 4, we have put constraints on NP contributions to the Wilson coefficients at a matching scale of $160\,\text{GeV}$. Here we give the relation to the effective Wilson coefficients at low energies, which are the quantities relevant for the evaluation of observables.

In low-energy observables, the coefficients C_7 and C_9 always appear in a particular combination with four-quark operators (which can be found e.g. in [19]) in matrix elements. It hence proves convenient to define effective coefficients $C_{7,9}^{\text{eff}}$, which are given by [104]

$$C_7^{\text{eff}} = C_7 - \frac{1}{3}C_3 - \frac{4}{9}C_4 - \frac{20}{3}C_5 - \frac{80}{9}C_6 \,, \tag{B.1}$$

$$C_9^{\text{eff}} = C_9 + Y(q^2) \,, \tag{B.2}$$

with

$$Y(q^2) = h(q^2, m_c)\left(\frac{4}{3}C_1 + C_2 + 6C_3 + 60C_5\right) \tag{B.3}$$

$$- \frac{1}{2}h(q^2, m_b)\left(7C_3 + \frac{4}{3}C_4 + 76C_5 + \frac{64}{3}C_6\right) \tag{B.4}$$

$$- \frac{1}{2}h(q^2, 0)\left(C_3 + \frac{4}{3}C_4 + 16C_5 + \frac{64}{3}C_6\right) + \frac{4}{3}C_3 + \frac{64}{9}C_5 + \frac{64}{27}C_6 \tag{B.5}$$

at leading order in α_s and Λ_{QCD}/m_b. Beyond the leading order, there are perturbative corrections as well as power corrections, which differ for inclusive and exclusive $b \to s\ell^+\ell^-$ decays. We refer the reader to refs. [44, 45, 47–51, 69, 74] for these corrections. Ref. [70] contains the expressions for the doubly Cabibbo-suppressed contribution to (B.1)–(B.2) which is relevant for the SM prediction of the $B \to K^*\mu^+\mu^-$ CP asymmetries.

In the SM, one finds at the scale $\mu_b = 4.8\,\text{GeV}$, to NNLL accuracy [55],

$$C_7^{\text{eff}}(\mu_b) = -0.304 \,, \qquad C_9(\mu_b) = 4.211 \,, \qquad C_{10}(\mu_b) = -4.103 \,, \tag{B.6}$$

while the primed coefficients are negligible. Beyond the SM, but assuming the four-quark operators to be free of NP, one has

$$C_7^{\text{eff}}(\mu_b) = C_7^{\text{eff,SM}}(\mu_b) + C_7^{\text{NP}}(\mu_b) \,, \tag{B.7}$$

$$C_9^{\text{eff}}(\mu_b) = C_9^{\text{eff,SM}}(\mu_b) + C_9^{\text{NP}} \,, \tag{B.8}$$

$$C_{10} = C_{10}^{\text{SM}} + C_{10}^{\text{NP}} \,, \tag{B.9}$$

$$C_7'(\mu_b) = C_7'^{\text{NP}}(\mu_b) \,, \tag{B.10}$$

$$C_{9,10}'(\mu_b) = C_{9,10}'^{\text{NP}} \,. \tag{B.11}$$

While the NP contributions to $C_9^{(\prime)}$ and $C_{10}^{(\prime)}$ do not run, $C_7^{(\prime)}$ do and they mix with $C_8^{(\prime)}$ under renormalization. With leading order running, as is appropriate for NP contributions evaluated at one loop, from a high matching scale $\mu_h = 160\,\text{GeV}$, one finds

$$C_7^{(\prime)\text{NP}}(\mu_b) = 0.623\, C_7^{(\prime)\text{NP}}(\mu_h) + 0.101\, C_8^{(\prime)\text{NP}}(\mu_h) \,. \tag{B.12}$$

Since the low-energy observables are sensitive to $C_7^{(\prime)\text{NP}}(\mu_b)$, the constraints we presented in sections 3 and 4 on $C_7^{(\prime)\text{NP}}(\mu_h)$ for vanishing $C_8^{(\prime)\text{NP}}$ can be interpreted as constraints on $C_7^{(\prime)\text{NP}}(\mu_h) + 0.162\, C_8^{(\prime)\text{NP}}(\mu_h)$ for non-standard $C_8^{(\prime)}$.

References

[1] A. Buras, P. Gambino, M. Gorbahn, S. Jager and L. Silvestrini, *Universal unitarity triangle and physics beyond the standard model*, *Phys. Lett.* **B 500** (2001) 161 [hep-ph/0007085] [INSPIRE].

[2] G. D'Ambrosio, G. Giudice, G. Isidori and A. Strumia, *Minimal flavor violation: An Effective field theory approach*, *Nucl. Phys.* **B 645** (2002) 155 [hep-ph/0207036] [INSPIRE].

[3] THE LHCB collaboration, B. Adeva et al., *Roadmap for selected key measurements of LHCb*, arXiv:0912.4179 [INSPIRE].

[4] T. Aushev et al., *Physics at Super B Factory*, arXiv:1002.5012 [INSPIRE].

[5] SUPERB collaboration, B. O'Leary et al., *SuperB Progress Reports — Physics*, arXiv:1008.1541 [INSPIRE].

[6] LHCB collaboration, *Angular analysis of $B^0 \to K^{*0}\mu^+\mu^-$*, LHCb-CONF-2011-038.

[7] C. Bobeth, G. Hiller and G. Piranishvili, *Angular distributions of $\bar{B} \to K\bar{l}l$ decays*, *JHEP* **12** (2007) 040 [arXiv:0709.4174] [INSPIRE].

[8] C. Bobeth, G. Hiller, D. van Dyk and C. Wacker, *The decay $B \to Kl^+l^-$ at Low Hadronic Recoil and Model-Independent $\Delta B = 1$ Constraints*, *JHEP* **01** (2012) 107 [arXiv:1111.2558] [INSPIRE].

[9] C. Bobeth et al., *Upper bounds on rare K and B decays from minimal flavor violation*, *Nucl. Phys.* **B 726** (2005) 252 [hep-ph/0505110] [INSPIRE].

[10] U. Haisch and A. Weiler, *Determining the Sign of the Z-Penguin Amplitude*, *Phys. Rev.* **D 76** (2007) 074027 [arXiv:0706.2054] [INSPIRE].

[11] T. Hurth, G. Isidori, J.F. Kamenik and F. Mescia, *Constraints on New Physics in MFV models: A Model-independent analysis of $\Delta F = 1$ processes*, *Nucl. Phys.* **B 808** (2009) 326 [arXiv:0807.5039] [INSPIRE].

[12] S. Descotes-Genon, D. Ghosh, J. Matias and M. Ramon, *Exploring new physics in the $C_7 - C_7'$ plane*, *JHEP* **06** (2011) 099 [arXiv:1104.3342] [INSPIRE].

[13] P. Gambino, U. Haisch and M. Misiak, *Determining the sign of the $b \to s\gamma$ amplitude*, *Phys. Rev. Lett.* **94** (2005) 061803 [hep-ph/0410155] [INSPIRE].

[14] C. Bobeth, G. Hiller and D. van Dyk, *The benefits of $\bar{B} \to \bar{K}^*l^+l^-$ decays at low recoil*, *JHEP* **07** (2010) 098 [arXiv:1006.5013] [INSPIRE].

[15] C. Bobeth, G. Hiller and D. van Dyk, *More benefits of semileptonic rare B decays at low recoil: CP-violation*, *JHEP* **07** (2011) 067 [arXiv:1105.0376] [INSPIRE].

[16] G. Hiller and F. Krüger, *More model independent analysis of $b \to s$ processes*, *Phys. Rev.* **D 69** (2004) 074020 [hep-ph/0310219] [INSPIRE].

[17] C. Bobeth, G. Hiller and G. Piranishvili, *CP asymmetries in $\bar{B} \to \bar{K}^*(\to \bar{K}\pi)\bar{\ell}\ell$ and untagged $\bar{B}_s$, $B_s \to \phi(\to K^+K^-)\bar{\ell}\ell$ decays at NLO*, *JHEP* **07** (2008) 106 [arXiv:0805.2525] [INSPIRE].

[18] C. Bobeth and U. Haisch, *New physics in Γ_{12}^s: $(\bar{s}b)$ $(\bar{\tau}\tau)$ operators*, `arXiv:1109.1826` [INSPIRE].

[19] C. Bobeth, M. Misiak and J. Urban, *Photonic penguins at two loops and m_t dependence of $BR[B \to X_s\ell^+\ell^-]$*, *Nucl. Phys.* **B 574** (2000) 291 [`hep-ph/9910220`] [INSPIRE].

[20] C. Bobeth, A.J. Buras, F. Krüger and J. Urban, *QCD corrections to $\bar{B} \to X_{d,s}\nu\bar{\nu}$, $\bar{B}_{d,s} \to \ell^+\ell^-$, $K \to \pi\nu\bar{\nu}$ and $K_L \to \mu^+\mu^-$ in the MSSM*, *Nucl. Phys.* **B 630** (2002) 87 [`hep-ph/0112305`] [INSPIRE].

[21] J. Laiho, E. Lunghi and R.S. Van de Water, *Lattice QCD inputs to the CKM unitarity triangle analysis*, *Phys. Rev.* **D 81** (2010) 034503 [`arXiv:0910.2928`] [INSPIRE]. Online update at www.latticeaverages.org.

[22] C. McNeile, C. Davies, E. Follana, K. Hornbostel and G. Lepage, *High-Precision f_{B_s} and HQET from Relativistic Lattice QCD*, *Phys. Rev.* **D 85** (2012) 031503 [`arXiv:1110.4510`] [INSPIRE].

[23] A.J. Buras, *Relations between $\Delta M_{s,d}$ and $B_{s,d} \to \mu\bar{\mu}$ in models with minimal flavor violation*, *Phys. Lett.* **B 566** (2003) 115 [`hep-ph/0303060`] [INSPIRE].

[24] LHCB collaboration, *Search for the rare decays $B^0_{(s)} \to \mu^+\mu^-$ with $300\,pb^{-1}$ at LHCb*, LHCb-CONF-2011-037.

[25] CMS collaboration, S. Chatrchyan et al., *Search for B_s and B to dimuon decays in pp collisions at $7\,TeV$*, Phys. Rev. Lett. **107** (2011) 191802 [`arXiv:1107.5834`] [INSPIRE].

[26] LHCB, CMS collaboration, *Search for the rare decay $B^0_s \to \mu^+\mu^-$ at the LHC with the CMS and LHCb experiments*, LHCb-CONF-2011-047.

[27] CDF collaboration, T. Aaltonen et al., *Search for $B_s \to \mu^+\mu^-$ and $B_d \to \mu^+\mu^-$ decays with CDF II*, *Phys. Rev. Lett.* **107** (2011) 239903 [`arXiv:1107.2304`] [INSPIRE].

[28] HEAVY FLAVOR AVERAGING GROUP collaboration, D. Asner et al., *Averages of b-hadron, c-hadron and τ-lepton properties*, `arXiv:1010.1589` [INSPIRE].

[29] M. Misiak et al., *Estimate of $B(\bar{B} \to X_s\gamma)$ at $O(\alpha_s^2)$*, *Phys. Rev. Lett.* **98** (2007) 022002 [`hep-ph/0609232`] [INSPIRE].

[30] M. Misiak and M. Steinhauser, *NNLO QCD corrections to the $\bar{B} \to X_s\gamma$ matrix elements using interpolation in m_c*, *Nucl. Phys.* **B 764** (2007) 62 [`hep-ph/0609241`] [INSPIRE].

[31] E. Lunghi and J. Matias, *Huge right-handed current effects in $B \to K^*(K\pi)\ell^+\ell^-$ in supersymmetry*, *JHEP* **04** (2007) 058 [`hep-ph/0612166`] [INSPIRE].

[32] D. Atwood, M. Gronau and A. Soni, *Mixing induced CP asymmetries in radiative B decays in and beyond the standard model*, *Phys. Rev. Lett.* **79** (1997) 185 [`hep-ph/9704272`] [INSPIRE].

[33] B. Grinstein, Y. Grossman, Z. Ligeti and D. Pirjol, *The photon polarization in $B \to X\gamma$ in the standard model*, *Phys. Rev.* **D 71** (2005) 011504 [`hep-ph/0412019`] [INSPIRE].

[34] P. Ball and R. Zwicky, *Time-dependent CP Asymmetry in $B \to K^*\gamma$ as a (Quasi) Null Test of the Standard Model*, *Phys. Lett.* **B 642** (2006) 478 [`hep-ph/0609037`] [INSPIRE].

[35] P. Ball, G.W. Jones and R. Zwicky, *$B \to V\gamma$ beyond QCD factorisation*, *Phys. Rev.* **D 75** (2007) 054004 [`hep-ph/0612081`] [INSPIRE].

[36] BELLE collaboration, Y. Ushiroda et al., *Time-dependent CP asymmetries in $B^0 \to K_S^0\pi^0\gamma$ transitions*, *Phys. Rev.* **D 74** (2006) 111104 [`hep-ex/0608017`] [INSPIRE].

[37] BABAR collaboration, B. Aubert et al., *Measurement of time-dependent CP asymmetry in* $B^0 \to K^0_S \pi^0 \gamma$ *decays*, *Phys. Rev.* **D 78** (2008) 071102 [arXiv:0807.3103] [InSPIRE].

[38] B. Meadows et al., *The impact of SuperB on flavour physics*, arXiv:1109.5028 [InSPIRE].

[39] J.M. Soares, *CP violation in radiative b decays*, *Nucl. Phys.* **B 367** (1991) 575 [InSPIRE].

[40] A.L. Kagan and M. Neubert, *Direct CP-violation in* $B \to X_s \gamma$ *decays as a signature of new physics*, *Phys. Rev.* **D 58** (1998) 094012 [hep-ph/9803368] [InSPIRE].

[41] M. Benzke, S.J. Lee, M. Neubert and G. Paz, *Long-distance dominance of the CP asymmetry in* $B \to X_{s,d} + \gamma$ *decays*, *Phys. Rev. Lett.* **106** (2011) 141801 [arXiv:1012.3167] [InSPIRE].

[42] BABAR collaboration, B. Aubert et al., *Measurement of the* $B \to X_s \ell^+ \ell^-$ *branching fraction with a sum over exclusive modes*, *Phys. Rev. Lett.* **93** (2004) 081802 [hep-ex/0404006] [InSPIRE].

[43] BELLE collaboration, M. Iwasaki et al., *Improved measurement of the electroweak penguin process* $B \to X_s \ell^+ \ell^-$, *Phys. Rev.* **D 72** (2005) 092005 [hep-ex/0503044] [InSPIRE].

[44] H. Asatrian, H. Asatrian, C. Greub and M. Walker, *Two loop virtual corrections to* $B \to X_s \ell^+ \ell^-$ *in the standard model*, *Phys. Lett.* **B 507** (2001) 162 [hep-ph/0103087] [InSPIRE].

[45] H. Asatryan, H. Asatrian, C. Greub and M. Walker, *Calculation of two loop virtual corrections to* $b \to s \ell^+ \ell^-$ *in the standard model*, *Phys. Rev.* **D 65** (2002) 074004 [hep-ph/0109140] [InSPIRE].

[46] C. Bobeth, P. Gambino, M. Gorbahn and U. Haisch, *Complete NNLO QCD analysis of* $\bar{B} \to X_s \ell^+ \ell^-$ *and higher order electroweak effects*, *JHEP* **04** (2004) 071 [hep-ph/0312090] [InSPIRE].

[47] A. Ghinculov, T. Hurth, G. Isidori and Y. Yao, *The Rare decay* $B \to X_s \ell^+ \ell^-$ *to NNLL precision for arbitrary dilepton invariant mass*, *Nucl. Phys.* **B 685** (2004) 351 [hep-ph/0312128] [InSPIRE].

[48] T. Huber, E. Lunghi, M. Misiak and D. Wyler, *Electromagnetic logarithms in* $\bar{B} \to X_s \ell^+ \ell^-$, *Nucl. Phys.* **B 740** (2006) 105 [hep-ph/0512066] [InSPIRE].

[49] Z. Ligeti and F.J. Tackmann, *Precise predictions for* $B \to X_s \ell^+ \ell^-$ *in the large* q^2 *region*, *Phys. Lett.* **B 653** (2007) 404 [arXiv:0707.1694] [InSPIRE].

[50] T. Huber, T. Hurth and E. Lunghi, *Logarithmically enhanced corrections to the decay rate and forward backward asymmetry in* $\bar{B} \to X_s \ell^+ \ell^-$, *Nucl. Phys.* **B 802** (2008) 40 [arXiv:0712.3009] [InSPIRE].

[51] C. Greub, V. Pilipp and C. Schupbach, *Analytic calculation of two-loop QCD corrections to* $b \to s \ell^+ \ell^-$ *in the high* q^2 *region*, *JHEP* **12** (2008) 040 [arXiv:0810.4077] [InSPIRE].

[52] K.S. Lee, Z. Ligeti, I.W. Stewart and F.J. Tackmann, *Universality and m(X) cut effects in* $B \to X_s \ell^+ \ell^-$, *Phys. Rev.* **D 74** (2006) 011501 [hep-ph/0512191] [InSPIRE].

[53] G. Bell, M. Beneke, T. Huber and X.-Q. Li, *Heavy-to-light currents at NNLO in SCET and semi-inclusive* $\bar{B} \to X_s l^+ l^-$ *decay*, *Nucl. Phys.* **B 843** (2011) 143 [arXiv:1007.3758] [InSPIRE].

[54] T.E. Browder, T. Gershon, D. Pirjol, A. Soni and J. Zupan, *New Physics at a Super Flavor Factory*, *Rev. Mod. Phys.* **81** (2009) 1887 [arXiv:0802.3201] [InSPIRE].

[55] W. Altmannshofer et al., *Symmetries and asymmetries of $B \to K^* \mu^+ \mu^-$ decays in the Standard Model and beyond*, *JHEP* **01** (2009) 019 [arXiv:0811.1214] [INSPIRE].

[56] U. Egede, T. Hurth, J. Matias, M. Ramon and W. Reece, *New observables in the decay mode $\bar{B}_d \to \bar{K}^{*0} \ell^+ \ell^-$*, *JHEP* **11** (2008) 032 [arXiv:0807.2589] [INSPIRE].

[57] BABAR collaboration, B. Aubert et al., *Angular distributions in the decays $B \to K^* \ell^+ \ell^-$*, *Phys. Rev.* **D 79** (2009) 031102 [arXiv:0804.4412] [INSPIRE].

[58] BELLE collaboration, J.-T. Wei et al., *Measurement of the Differential Branching Fraction and Forward-Backword Asymmetry for $B \to K^{(*)} \ell^+ \ell^-$*, *Phys. Rev. Lett.* **103** (2009) 171801 [arXiv:0904.0770] [INSPIRE].

[59] CDF collaboration, T. Aaltonen et al., *Measurement of the Forward-Backward Asymmetry in the $B \to K^{(*)} \mu^+ \mu^-$ Decay and First Observation of the $B_s^0 \to \phi \mu^+ \mu^-$ Decay*, *Phys. Rev. Lett.* **106** (2011) 161801 [arXiv:1101.1028] [INSPIRE].

[60] CDF collaboration, T. Aaltonen et al., *Measurements of the Angular Distributions in the Decays $B \to K^{(*)} \mu^+ \mu^-$ at CDF*, *Phys. Rev. Lett.* **108** (2012) 081807 [arXiv:1108.0695] [INSPIRE].

[61] F. Krüger and J. Matias, *Probing new physics via the transverse amplitudes of $B^0 \to K^{*0}(\to K^- \pi^+)\ell^+ \ell^-$ at large recoil*, *Phys. Rev.* **D 71** (2005) 094009 [hep-ph/0502060] [INSPIRE].

[62] A.K. Alok et al., *New-physics contributions to the forward-backward asymmetry in $B \to K^* \mu^+ \mu^-$*, *JHEP* **02** (2010) 053 [arXiv:0912.1382] [INSPIRE].

[63] E. Lunghi and A. Soni, *An improved observable for the forward-backward asymmetry in $B \to K^* \ell^+ \ell^-$ and $B_s \to \phi \ell^+ \ell^-$*, *JHEP* **11** (2010) 121 [arXiv:1007.4015] [INSPIRE].

[64] A.K. Alok et al., *New Physics in $b \to s \mu^+ \mu^-$: CP-Conserving Observables*, *JHEP* **11** (2011) 121 [arXiv:1008.2367] [INSPIRE].

[65] A.K. Alok et al., *New Physics in $b \to s \mu^+ \mu^-$: CP-Violating Observables*, *JHEP* **11** (2011) 122 [arXiv:1103.5344] [INSPIRE].

[66] U. Egede, T. Hurth, J. Matias, M. Ramon and W. Reece, *New physics reach of the decay mode $\bar{B} \to \bar{K}^{*0} \ell^+ \ell^-$*, *JHEP* **10** (2010) 056 [arXiv:1005.0571] [INSPIRE].

[67] A. Bharucha and W. Reece, *Constraining new physics with $B \to K^* \mu^+ \mu^-$ in the early LHC era*, *Eur. Phys. J.* **C 69** (2010) 623 [arXiv:1002.4310] [INSPIRE].

[68] A. Khodjamirian, T. Mannel, A. Pivovarov and Y.-M. Wang, *Charm-loop effect in $B \to K^{(*)} \ell^+ \ell^-$ and $B \to K^* \gamma$*, *JHEP* **09** (2010) 089 [arXiv:1006.4945] [INSPIRE].

[69] M. Beneke, T. Feldmann and D. Seidel, *Systematic approach to exclusive $B \to V \ell^+ \ell^-$, $V \gamma$ decays*, *Nucl. Phys.* **B 612** (2001) 25 [hep-ph/0106067] [INSPIRE].

[70] M. Beneke, T. Feldmann and D. Seidel, *Exclusive radiative and electroweak $b \to d$ and $b \to s$ penguin decays at NLO*, *Eur. Phys. J.* **C 41** (2005) 173 [hep-ph/0412400] [INSPIRE].

[71] P. Ball and R. Zwicky, *$B_{d,s} \to \rho, \omega, K^*, \phi$ decay form-factors from light-cone sum rules revisited*, *Phys. Rev.* **D 71** (2005) 014029 [hep-ph/0412079] [INSPIRE].

[72] B. Grinstein and D. Pirjol, *Exclusive rare $B \to K^* \ell^+ \ell^-$ decays at low recoil: Controlling the long-distance effects*, *Phys. Rev.* **D 70** (2004) 114005 [hep-ph/0404250] [INSPIRE].

[73] M. Beylich, G. Buchalla and T. Feldmann, *Theory of $B \to K^{(*)} \ell^+ \ell^-$ decays at high q^2: OPE and quark-hadron duality*, *Eur. Phys. J.* **C 71** (2011) 1635 [arXiv:1101.5118] [INSPIRE].

[74] D. Seidel, *Analytic two loop virtual corrections to $b \to d \ell^+ \ell^-$*, *Phys. Rev.* **D 70** (2004) 094038 [hep-ph/0403185] [INSPIRE].

[75] CKMFITTER GROUP collaboration, J. Charles et al., *CP violation and the CKM matrix: Assessing the impact of the asymmetric B factories*, *Eur. Phys. J.* **C 41** (2005) 1 [hep-ph/0406184] [INSPIRE]. Updated results and plots available at: http://ckmfitter.in2p3.fr.

[76] A. Bharucha, T. Feldmann and M. Wick, *Theoretical and Phenomenological Constraints on Form Factors for Radiative and Semi-Leptonic B-Meson Decays*, *JHEP* **09** (2010) 090 [arXiv:1004.3249] [INSPIRE].

[77] CDF collaboration, T. Aaltonen et al., *Observation of the Baryonic Flavor-Changing Neutral Current Decay $\Lambda_b^0 \to \Lambda \mu^+ \mu^-$*, *Phys. Rev. Lett.* **107** (2011) 201802 [arXiv:1107.3753] [INSPIRE].

[78] K.G. Chetyrkin, M. Misiak and M. Münz, *Weak radiative B meson decay beyond leading logarithms*, *Phys. Lett.* **B 400** (1997) 206 [*Erratum ibid.* **B 425** (1998) 414] [hep-ph/9612313] [INSPIRE].

[79] M. Gorbahn, U. Haisch and M. Misiak, *Three-loop mixing of dipole operators*, *Phys. Rev. Lett.* **95** (2005) 102004 [hep-ph/0504194] [INSPIRE].

[80] G. D'Agostini, *Asymmetric uncertainties: sources, treatment and potential dangers*, physics/0403086 [INSPIRE].

[81] W. Altmannshofer, A. Buras and P. Paradisi, *Low energy probes of CP-violation in a flavor blind MSSM*, *Phys. Lett.* **B 669** (2008) 239 [arXiv:0808.0707] [INSPIRE].

[82] R. Barbieri, P. Lodone and D.M. Straub, *CP violation in supersymmetry with effective minimal flavour violation*, *JHEP* **05** (2011) 049 [arXiv:1102.0726] [INSPIRE].

[83] R. Barbieri, G. Isidori, J. Jones-Perez, P. Lodone and D.M. Straub, *U(2) and minimal flavour violation in supersymmetry*, *Eur. Phys. J.* **C 71** (2011) 1725 [arXiv:1105.2296] [INSPIRE].

[84] R. Barbieri, P. Campli, G. Isidori, F. Sala and D.M. Straub, *B-decay CP-asymmetries in SUSY with a U(2)^3 flavour symmetry*, *Eur. Phys. J.* **C 71** (2011) 1812 [arXiv:1108.5125] [INSPIRE].

[85] A. Crivellin and L. Mercolli, *$B \to X_d \gamma$ and constraints on new physics*, *Phys. Rev.* **D 84** (2011) 114005 [arXiv:1106.5499] [INSPIRE].

[86] G. Isidori, Y. Nir and G. Perez, *Flavor Physics Constraints for Physics Beyond the Standard Model*, *Ann. Rev. Nucl. Part. Sci.* **60** (2010) 355 [arXiv:1002.0900] [INSPIRE].

[87] R. Barbier et al., *R-parity violating supersymmetry*, *Phys. Rept.* **420** (2005) 1 [hep-ph/0406039] [INSPIRE].

[88] D.M. Straub, *New physics correlations in rare decays*, arXiv:1012.3893 [INSPIRE].

[89] P. Langacker and M. Plümacher, *Flavor changing effects in theories with a heavy Z' boson with family nonuniversal couplings*, *Phys. Rev.* **D 62** (2000) 013006 [hep-ph/0001204] [INSPIRE].

[90] P. Langacker, *The Physics of Heavy Z' Gauge Bosons*, *Rev. Mod. Phys.* **81** (2009) 1199 [arXiv:0801.1345] [INSPIRE].

[91] A.J. Buras and L. Silvestrini, *Upper bounds on $K \to \pi\nu\bar{\nu}$ and $K_L \to \pi^0 e^+ e^-$ from ϵ'/ϵ and $K_L \to \mu^+\mu^-$*, *Nucl. Phys.* **B 546** (1999) 299 [hep-ph/9811471] [INSPIRE].

[92] G. Buchalla, G. Hiller and G. Isidori, *Phenomenology of nonstandard Z couplings in exclusive semileptonic $b \to s$ transitions*, *Phys. Rev.* **D 63** (2000) 014015 [hep-ph/0006136] [INSPIRE].

[93] W. Altmannshofer, A.J. Buras, D.M. Straub and M. Wick, *New strategies for New Physics search in $B \to K^* \nu\bar{\nu}$, $B \to K\nu\bar{\nu}$ and $B \to X_s \nu\bar{\nu}$ decays*, *JHEP* **04** (2009) 022 [arXiv:0902.0160] [INSPIRE].

[94] E. Lunghi, A. Masiero, I. Scimemi and L. Silvestrini, *$B \to X_s \ell^+ \ell^-$ decays in supersymmetry*, *Nucl. Phys.* **B 568** (2000) 120 [hep-ph/9906286] [INSPIRE].

[95] LHCB collaboration, *Combination of ϕ_s measurements from $B_s^0 \to J/\psi\phi$ and $B_s^0 \to J/\psi f_0(980)$*, LHCb-CONF-2011-056.

[96] Y. Grossman, Z. Ligeti and E. Nardi, *New limit on inclusive $B \to X_s \nu\bar{\nu}$ decay and constraints on new physics*, *Nucl. Phys.* **B 465** (1996) 369 [*Erratum ibid.* **B 480** (1996) 753-754] [hep-ph/9510378] [INSPIRE].

[97] D. Melikhov, N. Nikitin and S. Simula, *Right-handed currents in rare exclusive $B \to (K, K^*)\nu\bar{\nu}$ decays*, *Phys. Lett.* **B 428** (1998) 171 [hep-ph/9803269] [INSPIRE].

[98] M. Bartsch, M. Beylich, G. Buchalla and D.-N. Gao, *Precision Flavour Physics with $B \to K\nu\bar{\nu}$ and $B \to K\ell^+\ell^-$*, *JHEP* **11** (2009) 011 [arXiv:0909.1512] [INSPIRE].

[99] J.F. Kamenik and C. Smith, *Tree-level contributions to the rare decays $B^+ \to \pi^+ \nu\bar{\nu}$, $B^+ \to K^+ \nu\bar{\nu}$ and $B^+ \to K^{*+} \nu\bar{\nu}$ in the Standard Model*, *Phys. Lett.* **B 680** (2009) 471 [arXiv:0908.1174] [INSPIRE].

[100] A.J. Buras, K. Gemmler and G. Isidori, *Quark flavour mixing with right-handed currents: an effective theory approach*, *Nucl. Phys.* **B 843** (2011) 107 [arXiv:1007.1993] [INSPIRE].

[101] BABAR collaboration, P. del Amo Sanchez et al., *Search for the Rare Decay $B \to K\nu\bar{\nu}$*, *Phys. Rev.* **D 82** (2010) 112002 [arXiv:1009.1529] [INSPIRE].

[102] W. Altmannshofer, A.J. Buras, S. Gori, P. Paradisi and D.M. Straub, *Anatomy and Phenomenology of FCNC and CPV Effects in SUSY Theories*, *Nucl. Phys.* **B 830** (2010) 17 [arXiv:0909.1333] [INSPIRE].

[103] PARTICLE DATA GROUP collaboration, K. Nakamura et al., *Review of particle physics*, *J. Phys.* **G 37** (2010) 075021 [INSPIRE].

[104] A. Buras, M. Misiak, M. Münz and S. Pokorski, *Theoretical uncertainties and phenomenological aspects of $B \to X_s \gamma$ decay*, *Nucl. Phys.* **B 424** (1994) 374 [hep-ph/9311345] [INSPIRE].